CGILS: Results from the first phase of an international project to understand the physical mechanisms of low cloud feedbacks in single column models

Minghua Zhang,[1] Christopher S. Bretherton[2] Peter N. Blossey,[2] Phillip H. Austin,[3] Julio T. Bacmeister,[4] Sandrine Bony,[5] Florent Brient,[5] Suvarchal K. Cheedela,[6] Anning Cheng,[7] Anthony D. Del Oenio,[8] Stephan R. De Roode,[9] Satoshi Endo,[10] Charmaine N. Franklin,[11] Jean-Christophe Oolaz,[12] Cecile Hannay,[4] Thijs Heus,[6] Francesco Alessandro Isotta,[13] Jean-Louis Dufresne,[5] In-Sik Kang,[14] Hideaki Kawai,[15] Martin Koehler[16] Vincent E. Larson,[17] Yangang Liu[10] Adrian P. Lock,[18] Ulrike Lohmann[13] Marat F. Khairoutdinov,[1] Andrea M. Molod,[19] Roel A J. Neggers[20] Philip Rasch[21] Irina Sandu[6,16] Ryan Senkbeil,[17] A Pier Siebesma,[20] Colombe Siegenthaler-Le Drian,[13] Bjorn Stevens,[6] Max J. Suarez,[19] Kuan-Man Xu,[7] Knut von Salzen,[22] Mark J. Webb,[18] Audrey Wolf,[23] and Ming Zhao[12]

Received 6 June 2013; revised 31 October 2013; accepted 5 November 2013.

[1] COILS-the CFMIP-OASS Intercomparison of Large Eddy Models (LESs) and single column models (SCMs)-investigates the mechanisms of cloud feedback in SCMs and LESs under idealized climate change perturbation. This paper describes the COILS results from 15 SCMs and 8 LES models. Three cloud regimes over the subtropical oceans are studied: shallow cumulus cumulus under stratocwnulus, and well-mixed coastal stratus/stratocumulus. In the stratocumulus and coastal stratus regimes, SCMs without activated shallow convection generally simulated negative cloud feedbacks while models with active shallow convection generally simulated positive cloud feedbacks. In the shallow cumulus alone regime this relationship is less clear likely due to the changes in cloud depth lateral mixing and precipitation or a combination of them. The majority of LES models simulated negative cloud feedback in the well-mixed coastal stratus/stratocumulus regime, and positive feedback in the shallow cumulus and stratocwnulus regime. A general framework is provided to interpret SCM results: in a warmer climate, the moistening rate of the cloudy layer associated with the surface-based turbulence parameterization is enhanced; together with weaker

[1]School of Marine and Atmospheric Sciences, Institute for Terrestrial and Planetary Atmospheres, Stony Brook University, Stony Brook, New York, USA.
[2]Department of Atmospheric Sciences, University of Washington, Seattle, Washington, USA.
[3]Department of Earth and Ocean Science, University of British Columbia, Vancouver, British Columbia, Canada.
[4]National Center for Atmospheric Research, Earth System Laboratory, Boulder, Colorado, USA.
[5]Laboratoire de Meteorologie Dynamique/Lnstitute Pierre Simon Laplace (IPSL), Paris, France.
[6]Max Planck Institute for Meteorology, Hamburg, Germany.
[7]NASA Langley Research Center, Hampton, Virginia, USA.
[8]NASA Goddard Institute for Space Studies, New York, New York, USA.
[9]Department of Geoscience & Remote Sensing, Delft University of Technology, Delft, Netherlands.
[10]Brookhaven National Laboratory, Environmental Sciences Department, Upton, New York, USA.
[11]Centre for Australian Weather and Climate Research, Commonwealth Scientific and Industrial Research Organisation (CSIRO), Aspendale, Victoria, Australia.
[12]NOAA Geophysical Fluid Dynamics Laboratory, Princeton, New Jersey, USA.
[13]Swiss Federal Institlte of Technology, Zurich, Switzerland.
[14]School of Earth and Environmental Sciences, Seoul National University, Seoul, South Korea.
[15]Meteorological Research Institlte, Tsukuba, Japan.
[16]European Centre for Medium-Range Weather Forecasts, Reading, UK.
[17]Department of Mathematical Sciences, University of Wisconsin, Milwaukee, Wisconsin, USA.
[18]Met Office Hadley Centre, Exeter, UK.
[19]Global Modeling and Assimilation Office, NASA Goddard Space Flight Center, Greenbelt, Maryland, USA.
[20]Atmospheric Research Division, Royal Netherlands Meteorological Lnstitute (KNMI), De Bilt, Netherlands.
[21]Pacific Northwest National Laboratory, Richland, Washington, USA.
[22]Canadian Centre for Climate Modelling and Analysis, Victoria, British Columbia. Canada.
[23]Goddard Ln titlte for Space Stlldies, Columbia University, New York, New York, USA.
Corresponding author: M. Zhang, School of Marine and Atmospheric Sciences, Institlte for Terrestrial and Planetary Atmospheres, Stony Brook University, Stony Brook, NY 11794-5000, USA. (minghua.zhang@stonybrook.edu)

©2013. American Geophysical Union. All Rights Reserved. 1942-2466/13/10.1002/2013MS000246

large-scale subsidence, it causes negative cloud feedback. In contrast, in the warmer climate, the drying rate associated with the shallow convection scheme is enhanced. This causes positive cloud feedback. These mechanisms are summarized as the " ESTS" negative cloud feedback and the SCOPE" positive cloud feedback (Negative feedback from Surface Turbulence under weaker Subsidence-Shallow Convection PositivE feedback) with the net cloud feedback depending on how the two opposing effects counteract each other. The LES results are consistent with these interpretations.

Citation: Zhang, M., et al. (2013), CGILS: Results from the first phase of an international project to m1derstand the physical mechanjsms of low cloud feedbacks in single column models, *J. Adv. Model. Earth Syst., 5,* doi:10.1002/2013MS000246.

1. Introduction

[2] Cloud-climate feed backs in General Ci rcula tion Models (GCMs) have been the subject of intensive stud y for the last four decades [e.g., *Randall et al.,* 2007]. These feedbacks were iden tified to be one of the most significant uncertain ties in projecting future global warming in past IPCC (Inter-Governmental Panel for Climate Change) Assessment Reports (AR), as well as in coupled model sim ulations that will be used for the upcoming AR5 [*Andrews et al.,* 2012]. Despite much progress toward understanding cloud feed backs [*Bony et al.,* 2006], however, there is still a general lack of knowl edge a bou t thei r mechanisms . Understanding the physical mechanisms is necessary to increase our confidence in the sensi tivi ty estimates of climate models.

[3] Cloud-dinrnte feed backs refer to the radiative in1pact of changes of clouds on climate change. Because clouds are not explicitly resolved in GCMs, they are the product of an interactive and elaborate sui te of physical parameterization s. As a result, i t has been a challenge to decipher cloud feed back mechani sm s in climate models. Clouds also interact wi th the resolved-scale a tmospheric dynamical circulations through their impact on latent and radiative heating.

[4] In view of the challenges, CFMIP (the Cloud Feedback Model Intercomparison Project) and GASS (Global Atmospheric System Studies) initiated a joint project-CGILS (the CFMIP-GASS Intercomparison of Large Eddy Models (LESs) and single column models (SCMs)) to analyze the physical mechanisms of cloud feedbacks in SCMs by using an idealized experimental setup. The focus of CGILS is on low clouds in the subtropics, beca use several studies have demonstrated that these clouds contribute significantly to cloud feedback differences in models [e.g., *Bony and Dufresne,* 2005; *Zelinka et al.,* 2012]. The role played by these clouds is consistent with the fact that low cloud s have the largest net cloud-radiative effect, in contrast to deep clouds in which the positive longwave and negative shortwave cloud effects largely cancel out [e.g., *Ramm1athan et al.,* 1989].

[s] The objective of this paper is to describe the CGILS project and results from 15 SCMs and 8 LES models. Section 2 briefly descri bes the experimental design and large-scale forcing data. Section 3 gives a brief description of the partici pating model s. Section 4 discusses simulated clouds and the associated physical processes. Section 5 presents cloud feedback results . A brief sun1mary is given in Section 6.

2. Experimental Design and Large-Scale Forcing Data

2.1. Experimental Design

[6] The CGILS experimental design was described in *Zhang et al.* [2012], which is schematically shown in Figure 1. In t he control climate (CTL), sea surface tem perat ure (SST) is specified along the GCSS/WGNE Pacific Cross Section Intercomparison (GPCI) *[Teixeira et al.,* 2011] in the northeast Pacific by using the ECMWF (European Center for Medium-Range Weather Forecasts) Interim Reanalysis (ER A-Interim) [*Dee et al.,* 201 1] July 2003 condition as given in Ta ble I of *Zhang et al.* [2012]. In the pert urbed clima te, SST is uniformJ y raised everywhere by 2° as in *Cess et al.* [1990]. Large-scale horizontal advection and vertical motion , corresponding to the underlying SST, were derived and used to force SCMs and LES models. The perturbed climate is referred to as P2S, wi th "S" denotes that t he large-scale subsidence is also differen t from CTL *[Bretherton et al.,* 2013]. The models simulate changes of clouds in response to changes of SST and the associated large-scale atmospheric conditions.

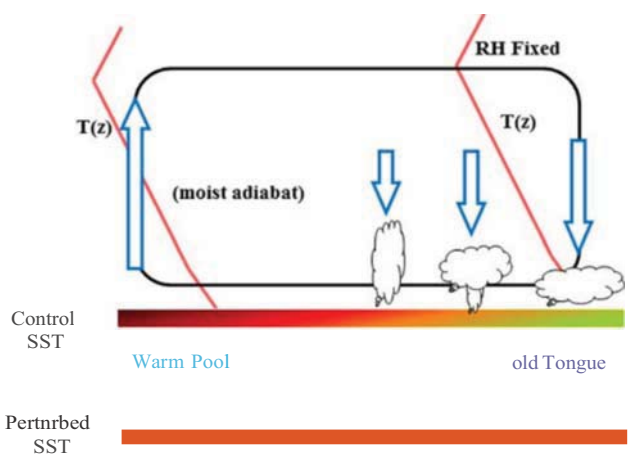

Figure 1. Schematics of the experimental setup . The atmospheric tem perature and wa ter vapor are constructed based on moist adiabat and fi xed relative h umidity, respecti vel y . The large-scale subsidence is calculated based on the clear-sky them1odynamic eq uation. These fields change wi th SST warming of 2°C in the perturbed climate.

Table 1. Participating Models, Main References, and Contributorsa

Models Acronyms	Model Institution	References	Contributors	Layers: Total/ (p > 700 hPa)
SCM (15)				
ACCESS (Australian Community Climate and Earth System Simulator)	Australian Commonweal th Scientific and Industrial Research Organisation/ Centre for A ustralian Weather and Climate Research	*Hew itel al.* [201 1J	Charmaine Franklin	38/12
CA M4 (Communiry Atmospheric Model Version 4)	National Center for Atmospheric Research (NCA R), USA	*Neale el al.* [201 OJ	Minghua Zhang, Cecile Hannay, and Philip Rasch	26/5
CA MS (Community A tmospheric Model Version 4)	National Center for Atmospheric Research (NCA R), USA	*Neale el al.* [2012J	Minghua Zhang, Cecile Hannay, and Philip R asch	30/9
CCC (Canadian Centre for Climate)	Canadian Centre for Climate Modell ing and Analysis, Canada	*Ma et al.* [2010]	Phillip Austi n and Knut von Salzen	35/14
CLUBB (Cloud Layers Unified By Binormals)	University of Wisconsin at Milwaukee, USA	*Goto= et of.* [2002a, 2002J, *LJHson and Galaz* [2005], and *Galaz el al.* [2007]	Vincent Larson and Ryan Senkbeil	41129
ECHAM6 (ECMWF-University of Ham burg Model Version 6)	Max-Planck Institute of Meteorology, Germany	*Ste1 1ens el al.* [2013J	Suvarchal Cheedela and Bjorn Stevens	31/9
ECMWF (European Center for Medium R ange Weather Forecasting)	European Center for Medium Ran ge Weather Forecasti ng	*Neggers et al.* [2009a, 2009bJ	Martin Koehler	91120
EC-ETH (ECMWF-Eidgenossische Technische H ochschule)	Swiss Federal I nstitute of Technology , Switzerland	*ll-otta et al.* [201 1J	Colombe Siegenthaler-Le Dri an, I sot ta Francesco Alessandro, and Ulrike Lohman	31/9
GFDL-AM3 (Geophysical Fluid Dynamics Lab oratory Atmospheric Model Version 3)	NOAA Geophysical Fl uid Dynamics Laboratory, USA	*Donner et al.* [201 1J	Jean-Christophe Golaz and Ming Zhao	48/12
GISS (Goddard In stitute for Space Sn1dies)	NASA Goddard Institute for Space Sn.dies, USA	*Schmidt et al.* [2006J	Anthony DelGenio and Audrey Wol f	40/9
GMAO (NASA Global Modeling and Assimilation Office)	NASA Goddard Space Flight Center, USA	*Rienecker et al.* [2008J and *Mofod et af.* (2012]	Andrea Molod, Max Suarez, and Julio Bacmeister	72/13
HadGEM2 (Hadl ey Centre Global Environment Model version 2)	Met Office, United Kin gdom	*Lock et al.* [2001] and *Mar tin et al.* [201 1J	Adrian Lock and Mark Webb	3811 2
JMA (Japan Meteorological Agency)	Japan Meteorological Agency, Japan	*Kawai* [2012J	Hideaki Ka wai	60/16
lPSL (Institute Pierre Simon Laplace)	Institute Pierre Simon Laplace (IPSL), France	*Hourdin et al.* [2006J	Florent Brient, Sandrine Bony, and Jean-Louis Dufresne	39/12
RA CMO (Regional Atmospheric Climate Model)	R oyal Netherlands Meteorological In stitute, the Netherlands	*Neggers et al.* [2009a, 2009bJ	Roel Neggers and Pier Siebesma	91120
LES (8)				
DALES (Dutch A tmospheric Large-Edd y Simulation)	R oyal Netherlands Meteorological Institute, the Netherlands	*Heus et al.* [20I OJ	Stephan de Roode	
LAR C (NASA Lan gley R esearch Center)	NASA Langley Research Cen ter, USA	*Xu et al.* [20I OJ	Anning Cheng and Kuan-man Xu	
SAM (System for Atmospheric Models)	University of Washington/ Stony Brook University, USA	*Klwirto11tdino 11 and Randaff* [2003J	Peter Bl ossey, Chris Bretherton, and Marat Khairoutdino v	
SAMA (System for A tmospheric Models)	University of Washington/ Stony Brook University, USA	*Khairto11tdino 11 and Randaff* [2003J and *Bfosse y et al.* [201 3J	Peter Bl ossey, Ch ris Bretherton, and Marat Khairoutdinov	
MOL EM (Met Office Large Eddy Model)	Met Office, United Kingdom	*Lock* [2009J	Adrian Lock	
MOL EMA (Met Office Large Eddy Model)	Met Office, United Kingdom	*Lo ck* [2009J and *Bfoss ey et al.* [2013]	Adrian Lock	
UCLA (University of California at Lo s Angeles)	Max Pl ank Institll te of Meteorology , Germany/ University of Ca lifornia at Lo s A ngeles, USA	*Ste1 1ens et al.* [2005J and *Ste vens and Seifert* [2008J	Thijs H eus, Irina Sandu, and Bjorn Stevens	

Table 1. (continued)

Models Acronyms	Model Institution	References	Contributors	Layers: Total/ (p > 700 hPa)
WRF (Weather Research and Forecasting)	National Center for Atmospheric Research/ Brookhaven National Laboratory	*Endo et al.* [2011]	Satosh End and Yangang Liu	

"The number of vertical layers and layers between the surface and 700 hPa for SCMs are given in the last column.

[7] Three locations along the GPCI cross section are selected for study. They are labeled as S6, Sl 1, and S12 in Figure 2, which also shows the distribution of low cloud amount in the sununer (JJA, June to August) from t he merged CALIPSO, CJ oudSat, CER ES, and MODIS satellite prod uct C3M [*Kato et al.,* 2011 ; *Xu and Cheng,* 2013]. Typical regimes of clouds at these three locations are shallow cumulus (S6), cumulus under stratocumulus (Sl 1), and well-mixed stratocumulus or coastal stratus (Sl 2). On the basis of dominant cloud types, they are referred to as shallow cum ul us, stratocumul us, and coastal strat us, respectively. The locations and val ues of summer-time surface meteorological variables in the control climate can be found in Table 1 of *Zhang et al.* [2012].

2.2. Forcing Data

[s] The SCM and LES forcing data refer to the Iarge-scale horizontal advective tendencies and vertical velocity, and surface bound ary condi tions that are specified in the model sim ulations. The SCMs calculate the time evol u tion of water vapor and temperature as follows [*Randall and Cripe,* 1999]:

$$\frac{\partial \theta}{\partial t} = -\omega \frac{\partial \theta}{\partial p} + \left(\frac{\partial \theta}{\partial t}\right)_{phys} - \omega_{LS}\frac{\partial \theta_{LS}}{\partial p}, \quad (1)$$

$$\frac{\partial q}{\partial t} = -\omega \frac{\partial q}{\partial p} + \left(\frac{\partial q}{\partial t}\right)_{phys} - \omega_{LS}\frac{\partial q_{LS}}{\partial p}. \quad (2)$$

where h and q are potential temperat ure and water vapor mixing ratio . Subscript *"m"* denotes model calculations ; *"LS"* stands for large-scale; other symbols are as commonly used. The first tem1 on the right-hand side (RHS) of equations (I) and (2) is calculated from physical parameterizations (with subscript *"phys").* The last two terms contain the specified large-scale horizontal advective forcing and subsidence. In LES models, conservative variables like liquid water potential temperature and total liquid water are typically used as prognostic fields [e.g., *Siebesma et al.,* 2004; *Stevens et al.,* 2005]. Equations (1) and (2) represent domain averages. The atmospheric winds and initial relative h umidity are specified by using the ERA-Interim for July 2003. Initial profiles of atmospheric temperature are assumed to follow moist adia bat over the warm pool and weak gradient approximations at other locations [*Sobel et al.,* 200 I]. Surface latent and sensi ble heat fluxes are calculated internally by each model from the specified SST and winds.

[9] The large-scale horizontal advective tendencies and subsidence in equations (1) and (2) are specified according to SST. In the free troposphere , they are deri ved based on the clear-sky thermodynamic and water vapor mass continuity equations , in which radiative cooling in the thermod ynamic equation is balanced by subsidence warming and horizontal ad vection, with the radiati ve cooling calculated by usi ng the RRTM radiation code [*Mlm ver et al.,* 1997] and the horizontal advection constrained by ERA-Interim. Below the altitude of 900 hPa, the horizontal advecti ve forcing of tem perature and water vapor are calcu lated using the SST spa tial gradient and specified surface relative h umidity. The detailed derivation of the CGILS forcing data and its comparison with the corresponding GCM and ER A-Interim can be found in *Zhang et al.* [2012].

[10] Figure 3a shows the derived vertical profiles of ω_{LS} in CGILS CTL (solid lines) and ERA -Interim (dashed lines) at the three chosen locations. The obtained values match well with ER A-Interim in the lower troposphere. Among the three locations, the subsidence rate is the strongest at S12 and the weakest at S6.

[1 1] Figure 3b shows the comparison of the derived ω_{LS} between CTL (solid lines) and P2S (dashed lines) used in the sim ulations. It is seen that subsidence is weaker in the warmer climate. Figures 3c and 3d show the corresponding profiles of horizontal advecti ve tendencies of tempera ture and water vapor, respectively. In the free troposphere, these profiles, along with

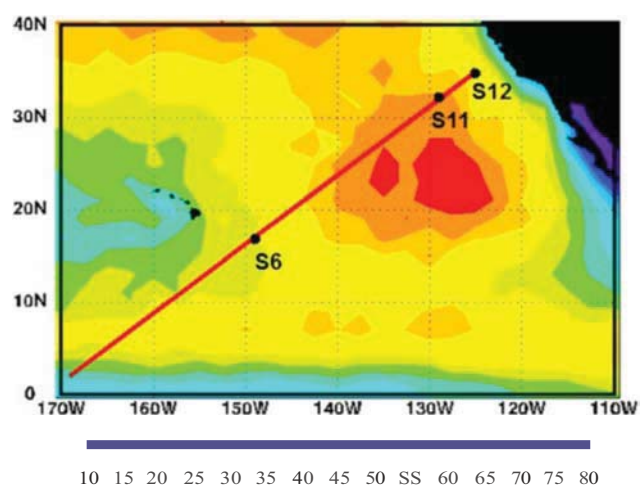

Figure 2. Averaged amount of low clouds in June-July-August (%) from the C3M satellite data. The red line is the northern por tion of the GPCI (see text); the symbols "S6," "Sll ," and "S12" are the three locations studied in the paper.

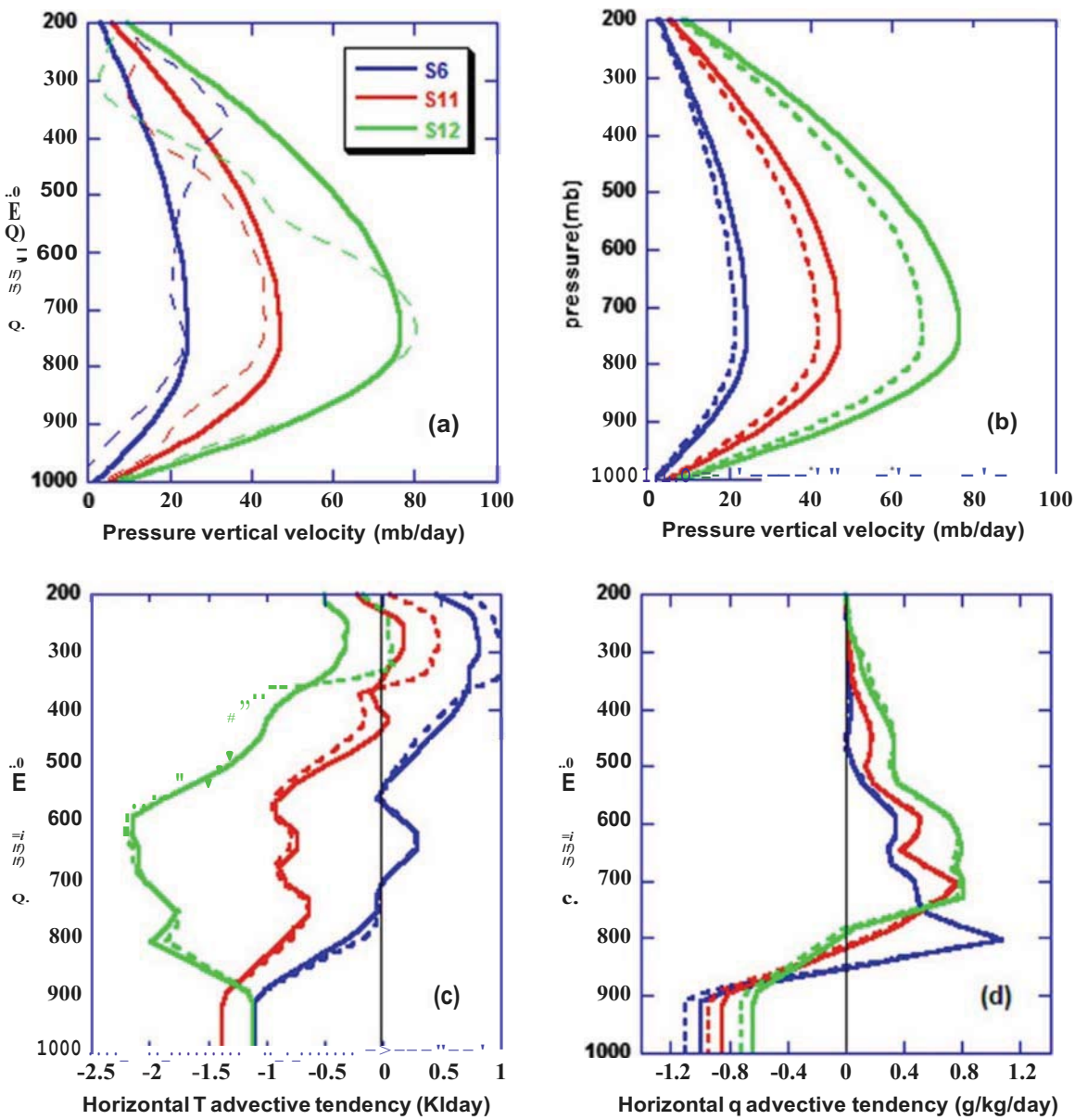

Figure 3. (a) Large-scale pressure vertical velocity at the three locations in the con trol dinrnte (solid lines), and in the ER A-Interim (dashed). (b) Same as Figure 3a except that the dashed l ines denote subsidence rates in the warmer climate. (c) Same as Figure 3b except for horizontal advective tendency of tem perat ure. (d) Same as Figu re 3c except for advective tendency of water vapor.

the profiles of $\times$ u;, SST, and initial atmospheric temperature and water vapor, satisfy the clear-sky atmospheric thermod ynamic and water vapor mass continuity eq uations under 15 July insolation conditions. *Zhang et al.* [2012] showed that the changes in the forci ng data between CTL and P2S in Figure 3 capture the essential features in GCMs . All data are available at the CGILS websi te http ://atmgcm.msrc.sunysb .edu/cfmip_ figs/Case_speci fication.html.

2.3. Simulations

[12] We use the change of cloud-radiative effect (CRE) from CTL to P2S, as in many previous studies, to measure cloud feed backs. Even though *Soden et al.* [2004] suggested other better diagnostics of cloud feedbacks, CR E is used for simplicity, which should not affect the results of this paper.

[13] The SCMs and LES are integrated to q uasi-equilibrium states by using the same steady large-scale advective tendencies and subsidence as forcing data. Each model ran six simulations: CTL and P2S a t the three locations of S6, S1 1 , and S 12. Since the forcing is fixed, a model may event ually d rift if its radiative cooling rate in the free a tmosphere d iffers from the rate used in the derivation of the prescribed large-scale subsidence. To prevent models from similar drifting, at

Table 2. Boundary-Layer Tw-bulence Schemes in SCMs

Models	R eferences	Local K_c	Cloud-top Entrai nment	Cotmter Gradient c_c
ACCESS	*Lock et al.* [2000]	N	y	y
CA M4	*Holtslag and Ba1•ille* [1993]	N	N	y
CAMS	*Br etherton and Park* [2009]	y	y	N
CCC	*1•0J1 Sa1en et al.* [2013]	y	y	y
CLUBB	*Galaz et al.* [2002a, 2002], *Larson and Galaz* [2005], and *Galaz et al.* [2007]	N	N	N
ECHAM6	*Ste1•ens et al.* [2012)	y	N	N
ECMWF	*Neggers et al.* [2009a, 2009b] and *Lock* [2000]	N	y	y
EC-ETH	*Brinkop and Roeckn er* [1995]	y	N	N
GFDL-AM3	*Lock et al.* [2000) and *Louis and Geleyn* [1982)	N	y	N
GISS	*Holtslag and Moeng* [1991) and *Del Genia et al.* [1996]	y	y	y
GMAO	*Lock et al.* [2000) and *Louil·and Geleyn* [1982)	N	y	y
HadGEM2	*Lock et al.* [2000]	N	y	y
JMA	*Mel/or and Yamada* [1974] and *Ka111ai* [2012]	y	N	N
rPSL	*Hourdin et al.* [2006]	y	N	y
RA CMO	*Neggers et al.* [2009a, 2009b]	N	y	y

pressure less t han 600 hPa , temperatu re and water vapor mixing ratio are relaxed to thei r initial conditions wi th a time scale of 3 h. In LES models , they are relaxed a t altitudes above 4000 m for S6, 2500 m for Sl 1, and 1200 m for S12, respectively, to reduce computational costs and allow for high vertical resolu tions in shallow domains. Some LES models did not com plete all six sim ulations.

[1 4] Most of the SCMs are integrated for 100 days. Based on a visual inspection of statistical eq uili brium, the averages of their last period of about 50 days are used . Most LES simulations reached quasi-equilibrium sta tes after l0 days, in which case the last 2 d ays are used in the analysis. *Zhang and Br etherton* [2008] analyzed the transient behavior of the Comm uni ty Atmospheric Model (CAM) under constant forcing and showed that the interaction of djfferent physical parameterization com ponents can create quasi-periodic behavior s of model sinm lation wi th time scales longer than a day. Since LES models contain fewer parameterization com ponents, the in1pact of this type of interactions is reduced , wruch may explain why LES models reach quasi steady states in shorter time than SCMs. To our knowled ge, CGILS is the first LES intercom parion stud y to investigate clouds by integra ting t hem to q uasi-eq uilibrium states.

3. Models and Differences in Physical Parameterizatio ns

[1 s] Fifteen SCMs and eight LES models pa r ticipated in this study. Many parent GCMs of the SCMs also par ticipated in the Coupled Model Intercomparison Project 5 (CMIP5) . Table 1 lists the model names , main references, and CGILS contri bu tors. It also gives the num ber of total vertical model layer s and n um ber of layers between the surface and 700 hPa in SCMs. The SCM vertical resol ution in the boundary layer (PBL) is generally not sufficient to resolve the observed or LES simulated thin stratocumulus clouds. No attempt is made to make them finer since our objective is to understand the behavior of operational GCMs. For the LES mod els, however, because they are intended as benchmarks, much higher resolutions are used . The horizontal resolutions of LES models are 100 m, 50 m, and 25 m, respecti vely, at S6, S 11, and S 12. The vertical resolutions of the majori ty of LES are 40 m, 5 m, and 5 m, respectively, at the th ree locations. More detailed descriptions of the CGILS LES models are given in a companion paper by *Blossey et al.* [2013].

[16] The physical parameterizations in the SCMs relevant to the present stud y are the PBL, shallow convection, and cloud schemes. For PBL schemes, the generic form can be wri tten in terms of t urbulent flux a t the mod el interfaces:

$$\overline{w'S'} = -K_c \frac{\partial S}{\partial z} + c_c \; ; \tag{3}$$

where z is height, w is vertical velocity, S is a conservative model prognostic variable. Prime represents the turbu lent perturbation from the mean that is denoted by the overbar. K_c is the eddy diffusivi ty, and c_c is the counter-gradient transport tem1. In addi tion to resol u-tion, the differences in PBL schemes among the models are in their formulations of K_c and c_c. For K_c, some mod els parameterize i t by using local variables a t the resolved scales, such as local Richardson num ber in the so-called fi rst order closure models, or local turbulent edd y k inetic energy (TKE) [*Mellor and Yamada,* 1974]. Other models use nonlocal em pirical parameterization of K_c as a function of heigh t relative to the boundary layer depth. Another K_c difference among the models is its parameterization at the top of the PBL. While some mod els have explicit parameterizations of turbulent entrainment based on parameters such as cloud -top radiative and evaporative cooling, others do not consider entrainment. For the counter-gradient tem1 c_c, some models calculate i t based on surface buoyancy fluxes, while others do not have this term. Table 2

Table 3. Shallow Convection Schemesa

Models Acronyms	References	Trigger	Lateral Entrainment	Lateral Detrainmen t	Closure
ACCESS	*Gregory and Ro11111tre e* [1990) and *Grant* [200l)	Undiluted parcel	Specified	Specified	TKE
CA M4	*Hack* [1994]	Undiluted parcel	N	N	CAPE
CA MS	*Park and Bretherton* [2009]	CIN 1TKE	Bu oyancy sorting	Bu oyancy sorting	CIN 1TKE
CCC	110U *Salzen et al.* [201 2], *van Salzen and McFarlane* [2002], and *Grant* [2001)	Undiluted parcel	Bu oyancy profile	Buoyancy profile	TKE
CLUBB	*Galaz et al.* [2002a, 2002), *Larson and Galaz* [2005), and *Galaz el al.* [2007)	N	N	N	High-order bi-normal distribution
ECHAM6	*Tiedtke* [1989)	Diluted parcel	Specified	Specified	Moisture con vergence
ECMWF	*Tiedtke* [1989)	Diluted parcel	Specified	Dia gnosed	Subcloud moist static energy
EC-ETH	*Von Salzen and McFarlan e* [2002), *Grant* [2001), and *lsotta el al.* [201 1)	Undiluted	Bu oyancy profile	Buo yancy profile	TKE
GFDL-AM3	*Bret herton and Park* [2009) and *Zhao et al.* [2009)	CIN 1TKE	Buo yancy sorti ng	Buoyancy sorting	CTN 1TKE
GISS	*Del Genia and Yao* [1993) and *Del Genia et al.* [2007)	Undiluted parcel	Bu oyancy and speed	Above neutral level	Cloud-base buoyancy
GMAO	*Moorthi and Suarez* [1992]	Undiluted	Di agnosed	N	CAPE
HadGEM2	*Gregory and Ro ivnlree* [1990) and *Grant* [200l]	Undiluted parcel	Specified	Specified	TKE
JMA	*Pan and Randall* [1998)	Diluted parcel	Di agnosed	N	Prognostic
IPSL	*Emanuel* [1991, 1993]	Undiluted parcel	Buo yancy sorti ng	Buoyancy sorting	CAPE
RACMO	*Neggers et al.* [2009a, 2009b]	Unified with PBL scheme	Unified wi th PBL scheme	Unified with PBL scheme	Unified wi th PBL scheme

"Some models use the same schemes for deep convections.

categorizes the PBL schemes in the SCMs accord ing to the above at tributes. Cloud-top entrainment in Table 2 refers to explicit parameterization . PBL schemes form u-lated using moist conserved variable and TKE closure (such as ECHAM6) may implicitly contain cloud-top entrainment. As can be seen, a wide variety of PBL parameterizations are used in the SCMs. Because of coarse vertical resolutions , however , some of these dif-ferences d o not make as m uch of an impact on cloud sim ulations as they would if higher vertical resol utions were used.

[1 l] The majori ty of SCMs used mass-flux shallow convection schemes. The generic fom1 of convective transport for a conservati ve variable q_1 i n these schemes is

$$\overline{w'q_t'} 5 M(z)(q_{tc} 2 q_{te}); \quad (4)$$

where the prime denotes deviation of the bul k proper-ties of clouds from the mean ; M is the convective mass flux; subscripts c and e represent values in the parame-terized cloud model and in the environment air, respec-tively. The convective mass flux is calculated from parameterized rates of en trainment and detrainment d

$$\frac{\partial M}{\partial z} 5 k2 cl:$$

[1s] Some models do not separatel y parameterize shallow and deep convection. The schemes can differ in their entrainment and detrainment rates, the closure that determines the amount of cloud base mass flu x, and convection triggering condition as well as origina-tion level of convection. Table 3 categorizes the convec-tive schemes in the SCMs based on these mai n attrib utes. Among the SCMs, CLUBB, and R ACMO use a single scheme to parameterize PBL turbulence and shallow convection.

[19] Cloud schemes in SCMs i nclude a macrophysical and a microphysical com ponent. Cloud macro physica l schemes parameterize cloud amount and the grid-scale rate of condensation and evaporation. These schemes can be generically described by assuming that the total water in the air, q_1, obeys a probability distribution function (pdl) $P(q_1)$ within a model grid box. The cloud amoun t is then

$$CS \quad P(q1)dq1; \quad (5)$$

where qs is the saturation vapor pressure at cloud tem-perature. Cloud liquid water $q1$ is then

$$q, 5 \quad (q12 qs) P(q1)dq1: \quad (6)$$

[20] Therefore, cloud fraction and cloud liquid water are often propor tional to each other in individ ual mod-els when the cloud fraction is less than 100%. The cloud microphysics scheme treats how condensed water is converted to precipi tation. In most parameterizations ,

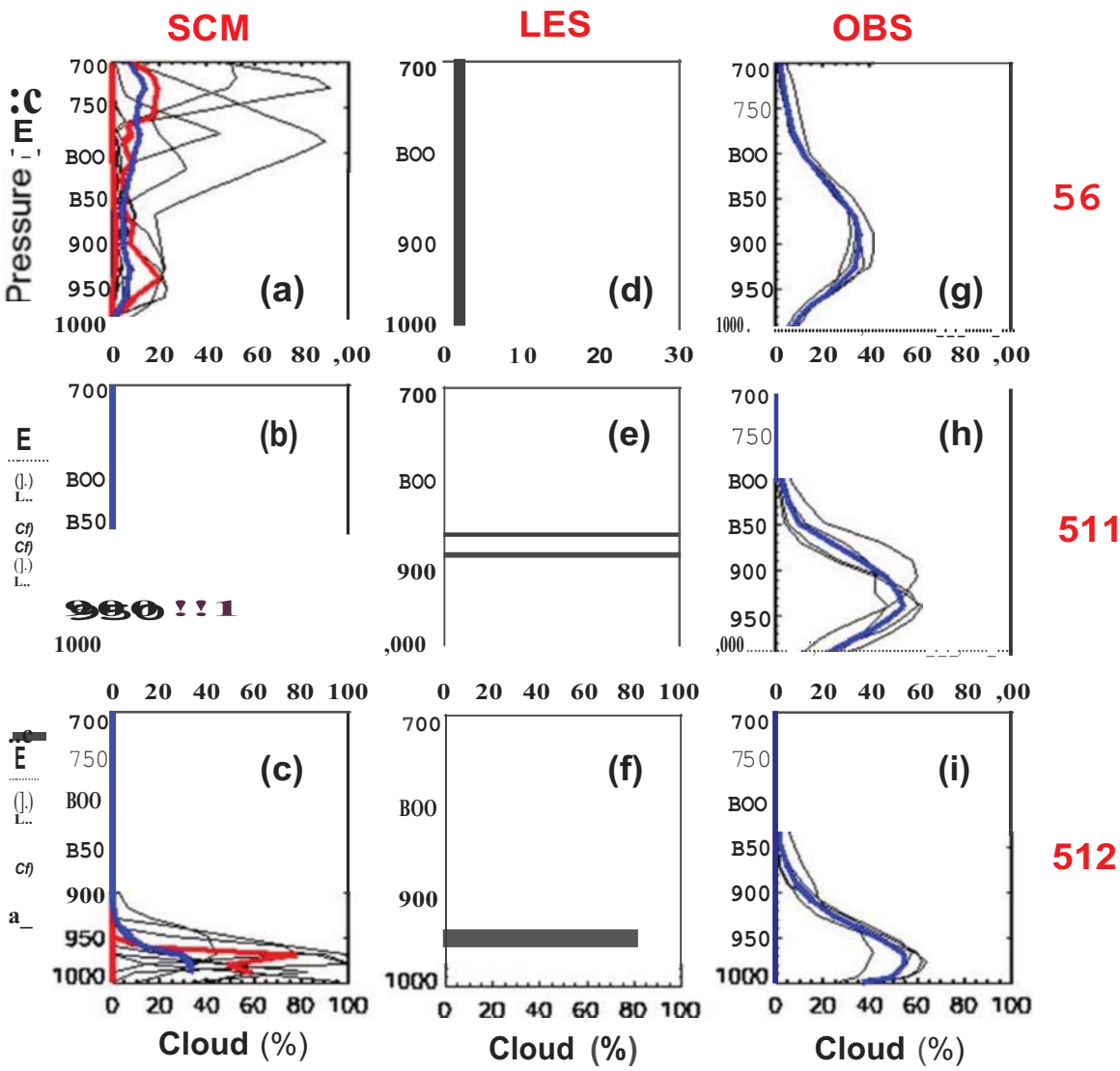

Figure 4. (a-c) Averaged profiles of cloud amount (%) by SCMs for S6, SI 1, and Sl 2, respectively (from top to bottom plots). (d-f) Same as Figures 4a-4c but by the LES models. (g-i) From the C3M satellite measurements. The blue lines are ensemble averages; the red lines are the 25% and 75% percentiles.

precipitation is typically proportional to cloud water, which is further proportional to rate of large-scale condensation.

4. Simulated Clouds and Associated Physical Processes

[21] Before investigating cloud feedbacks, we first examine the simulated clouds in CTL. Figure 4 shows the time-averaged cloud profiles in all 15 SCMs and all LES models, with the shallow cumulus location S6 in the top row and the stratus location S12 in the bottom row. SCMs results are in the left column; LES models in the middle column; observations from C3M for the summers of 2006-2009 in the right column. Note that the observations may have categorized drizzle as clouds, therefore having a different definition of clouds from that in the models. The blue lines denote the ensemble averages or multiyear averages; the red lines denote the 25 and 75 percentiles. Figure 5 shows examples of the time-pressure cross sections of these cloud amount from a sample of three SCMs (JAM, CAM4, and GISS), which are selected because they span the range of model differences as will be shown later, and from one LES (SAMA).

[22] Despite large differences among the models, the relative rank of cloud-top height and cloud amount at the three locations is correct. The spread in the LES models is much smaller than that among the SCMs. At S11, LES models simulated cumulus under stratocumulus. The use of the steady forcing for all models may have amplified the intermodel differences, since in both GCMs and the real atmosphere the large-scale circulation can respond to local differences in the inversion

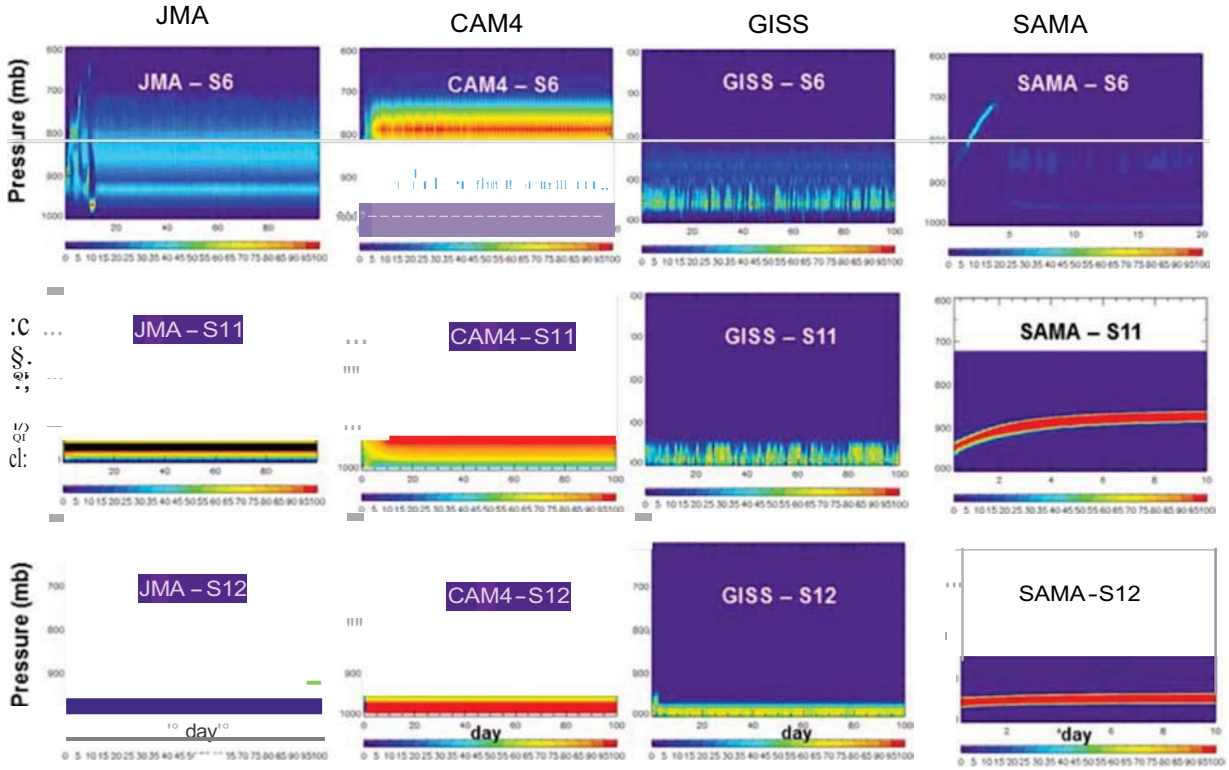

Figure 5. Examples of time evolution of cloud amount (%) simulated by JMA (left column) for S6, S11, and S12, respectively, from top to bottom plots; CAM4 (middle column); GISS (third column); SAMA (right column).

height by partially compensating them [*Blossey et al.*, 2009; *Bretherton et al.*, 2013].

[23] We find it instructive to use the following moisture budget equation to probe the physical parameterizations responsible for the simulated clouds in the SCMs. It is written as:

$$\frac{\partial q_v}{\partial t} = \frac{\partial q_v}{\partial t}\Big|_{turb} + \frac{\partial q_v}{\partial t}\Big|_{conv} + \frac{\partial q_v}{\partial t}\Big|_{c\text{-}e} + \frac{\partial q_v}{\partial t}\Big|_{LS} \qquad (7)$$

where the variables are as commonly used, and the tendency terms have been separated into three physical terms representing parameterizations of PBL turbulence (*turb*), convection (*conv*), large-scale stratiform net condensation (c-e), plus the three-dimensional large-scale forcing. As will be shown later, the separation of the physical tendency terms helps to provide a framework of interpreting cloud feedback behaviors in the models. We show the three selected models in Figure 6 of the time-averaged profiles of these three terms at S11 in CTL by using the colored solid lines. The black lines are the simulated grid-box mean cloud liquid water. The solid dots on top of the black lines donate the midpoint of model layer.

[24] In the JMA model, only two physical terms are active (Figure 6a) in addition to the large-scale dynamic forcing. The PBL scheme moistens the boundary layer; the large-scale condensation dries it. The residual is balanced by the drying from the large-scale forcing. The peak altitudes of the *"turb"* and *"c-e"* are the same as that of the cloud liquid water. Since the PBL scheme is always active, the stratiform condensation scheme responds to the PBL scheme. In CAM4, Figure 6b shows that shallow convection is active in addition to the *"turb"* and the *"c-e"* terms. The shallow convective scheme transports the moisture from the boundary layer to the free troposphere. In the GISS model, Figure 6c shows that shallow convection is also active, but unlike CAM4, the maximum drying of the *"conv"* term is at the same level as the maximum level of *"turb,"* in the middle of the cloud layer. These differences will be shown later as causes of different cloud feedbacks in the models. In Figure 6, the stratiform condensation term is the direct source of cloud water.

[25] The intermodel differences in Figure 6 are examples of how different parameterization assumptions can affect the balance of the physical processes and associated clouds. The JMA model used the prognostic Arakawa-Schubert convection scheme [*Pan and Randall*, 1998] with fixed cloud base level near 900 hPa in the model [*JMA*, 2013]. As a result, convection is not active in this case. CAM4 and GISS both used positive Convective Available Potential Energy (CAPE) of undiluted air parcels as criteria of convection. As a result, shallow convection is more easily triggered in these two

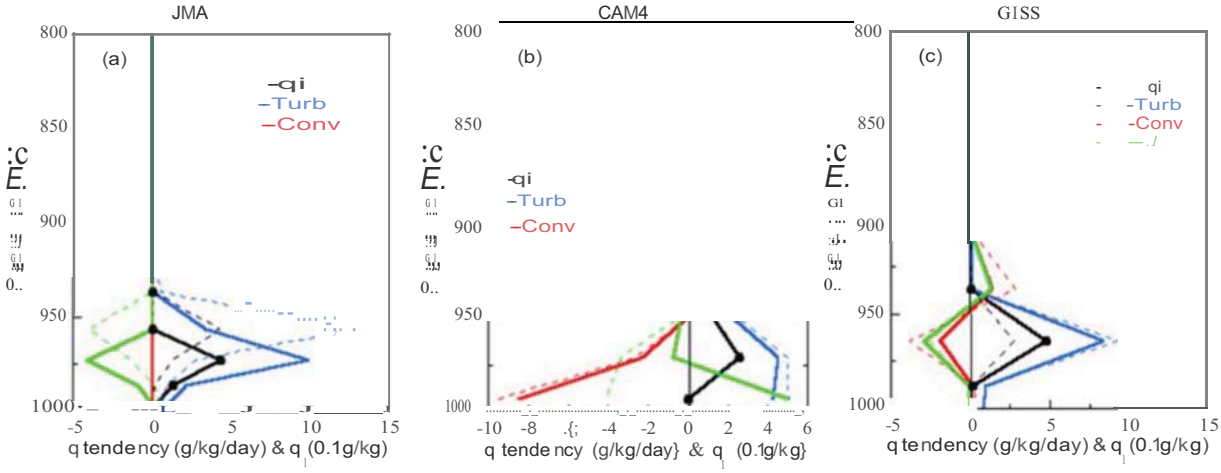

Figure 6. Solid lines are physical tendencies of water vapor (g/kg/day) in three SCMs a t Sl 1 for the control climate , *"turb"* for turbulence scheme, *"conv"* for convection scheme, *"(c-e)"* for net large-scale condensa tion , and *"qf"* for the grid-box cloud liquid water (0.1 g/kg) . The black dots show the mid point of model layers . The dashed lines show the correspondin g values in the warmer climate. (a) JMA, (b) CAM4, and (c) GISS.

models . Nevertheless, the assumptions in their shallow convection parameterizations are different. For example, CA M4 does not incl ud e lateral entrainment into the convective pl umes *[Ha ck ,* 1994], while GISS ha s lateral entrainment *[Del Genio and Yao,* 1993].

[26] Tables 4-6 show the simulated surface sensible and latent fluxes, precipitation , cloud water path , and cloud-radiative effects in the SCMs at Sl 2, Sll , and S6, respecti vely, in the control climate. Total cloud amount is not incl uded in the ta ble since in some models it is contaminated by unreali stic optically thin clouds in the upper troposphere. The expected increase of surface latent heat fluxes from S12 to SI 1 and S6 is simulated in most models. However , consistent wi th wha t has been shown in the vertical profiles of clouds in Figure 4, the models differ greatly in their cloud liquid water path, and as a result, in the shortwave cloud radiation effect. At S12, some models did not simulate clouds. As shown in *Zhang et al.* (2012] for the GFDL model, this unrealistic behavior is related to the use of steady forcing. When compared with the LES results of Tables 3-5 in *Blossey et al.* (2013], the SCM surface latent heat fluxes are generally smaller than in the LES models. This is likely related to the use of the steady forcing or insufficient entrainment mixing in the SCMs. The precipitations and the cloud liquid paths in the SCMs span a wide range that brackets the corresponding range in the LES models. Since the objective of CGILS is to investigate the cloud feedback or the response of the cloud fields to a warmer climate, we only use Figure 6

Table 4. Simulated ields in Control Climate and Their Changes in the Perturbed at S12 in SCMsa

Model_ID	SH	LH	PREC	TGLWP	SWCRF	CRE
ACCESS	13.8 (2 5.8)	58.9 (2 2.8)	0.00 (0.00)	14.2 (2 5.4)	2 79.4 (35.4)	2 72.2 (32.3)
CAM4	24. 7 (2 0.6)	48.3 (4.6)	0.00 (0.00)	199.4 (1 1.0)	2 210.4 (2 0.6)	2 21 5.5 (2 l.0)
CA MS	2 6.0 (0.2)	2.9 (0.3)	0.00 (0.00)	0.0 (0.0)	0.0 (0.0)	0.0 (0.0)
CCC	26.6 (2 3.6)	54.4 (13.1)	0.51 (2 0.14)	186.2 (2 82.5)	2 100.4 (17.2)	2 100.3 (19.5)
CL UBB	25.8 (2 1.6)	64.7 (11.4)	0.00 (2 0.00)	77.8 (24.2)	2 176.2 (2 18.2)	2 170.5 (2 18.0)
ECHAM6	2 22.8 (1.9)	62.2 (2.9)	1.10 (0.10)	98.1 (0.9)	2 121.4 (0.8)	2 124.1 (1.6)
ECMWF	10.1 (2 3.7)	68.1 (15.4)	0.00 (2 0.00)	12.5 (3.8)	9.9 (2 5.4)	12.8 (2 4.2)
EC_ETH*	2 27.9 (43.7)	1.5 (32.8)	0.00 (0.0)	0.0 (0.0)	0.0 (0.0)	0.0 (0.0)
GFDL_AM3	2 4.8 (1.1)	18.9 (2.6)	0.00 (0.00)	0.0 (0.0)	0.0 (0.0)	0.0 (0.0)
GISS	l1.3 (2 0.5)	59.9 (10.7)	0.35 (0.22)	140.9 (95.1)	2 l09.0 (2 24.5)	2 108.2 (2 24.3)
GMAO	1 .3 (0.2)	35.5 (2.1)	0.50 (2 0.50)	0.8 (2 0.8)	2 LO (0.9)	2 1.3 (1.2)
HadGEM2	17.0 (2 1.8)	61.2 (7.2)	0.70 (2 0.30)	23.9 (2 4.4)	2 95.5 (13.5)	2 88.7 (13.4)
IPSL	25.0 (2 1.6)	66.4 (5.4)	0.72 (0.80)	47.1 (0.3)	2 65.1 (0.0)	2 66.4 (0.5)
JMA	27.0 (2 0.4)	62.3 (4.9)	0.31 (0.70)	48.7 (7.2)	2 122.8 (2 8.4)	2 122.4 (2 8.5)
RACMO	20.2 (2 3.5)	68.2 (11.9)	0.40 (2 0.20)	34.3 (8.1)	2 33.4 (2 6.2)	2 27.6 (2 6.2)

"Numbers in the parentheses are the changes in the pertmbed climate. Listed are sensi ble and latent heat fluxes (SH, LH , in W/m2J, precipitation (PR EC, mm/day) , total cloud water path (TGLWP , g/m^2), sh ortwave, and total cloud-radiative effect (SWCRE , CR E, W/m^2). The ast erisk denotes that the model has not reached equilibri um state (the EC_ETH model).

Table 5. Same as Table 4 but for Si I

Model_lD	SH	LH	PR EC	TGLWP	SWCR E	CR E
ACCESS	1 1.9 (2 1.8)	84.1 (7.4)	0.26 (0.50)	65.0 (2 I0.8)	2 123.0 (29.1)	2 1 13.9 (26.4)
CA M4	23.7 (0.4)	59.3 (7.9)	0.00 (0.00)	77.2 (4.8)	2 133.4 (2 1.7)	2 129.7 (2 1.4)
CAM S	15.1 (2 0.3)	90.2 (9.1)	0.00 (0.20)	55.0 (14.9)	2 124.1 (2.3)	2 1 16.4 (2.8)
CCC	29. 7 (2 4.4)	63.3 (22.8)	0. 70 (2 0.33)	228.2 (2 76. 8)	2 107.2 (14.8)	2 100.8 (1 7.4)
CL UBB	4.2 (0.7)	88.5 (8.2)	0.00' (0.00)	25. 3 (6.3)	2 95.7 (2 14. 7)	2 78.5 (2 13.6)
ECHAM6	2 21.4 (1.7)	78.4 (5.6)	1 .33 (0. 90)	173.1 (3.0)	2 1 50.8 (0.4)	2 1 50.9 (0.7)
ECMWF	6.8 (2 0.6)	87.2 (1 2.3)	0.80 (0.13)	48.7 (15.1)	2 24.6 (2 7.2)	2 17.3 (2 6.3)
EC_ETH	6.5 (5.3)	73.1 (1 5.4)	0.31 (0.39)	144.4 (35.0)	2 129.4 (2 7.1)	2 130.1 (2 3.5)
GFDL_A M3	15.5 (2 6.3)	78. 7 (1 5.8)	0.30 (0.50)	40.0 (5.5)	2 118.4 (2 11.8)	2 111.3 (2 11.2)
GISS	1 0.8 (0.5)	76.3 (5.4)	0.43 (2 0.07)	129.8 (2 55.7)	2 68.1 (25.8)	2 66.2 (25.1)
GMAO	5.1 (2 0.1)	84.9 (8.0)	0.70 (0.11)	IO.O (10.7)	2 1 1.8 (2 9.8)	2 I0.2 (2 8.2)
HadGEM2	7.4 (2 0.2)	69.7 (5.3)	0.00 (2 0.00)	4.7 (2 3.3)	2 27.3 (9.4)	2 24.5 (8.7)
IPSL	23. 5 (2 0.9)	74.7 (7.6)	0.76 (0.1 1)	52.2 (-0.0)	2 69.3 (0.4)	2 63.5 (0.7)
JMA	26.9 (2 4.1)	73. I (14.5)	0.59 (0.50)	80.3 (20.1)	2 157.1 (2 13.9)	2 151.5 (2 15.4)
RA CMO	15.3 (2 2.3)	91.0 (8.9)	0.24 (2 0.18)	1 00.9 (2 5.5)	2 85.7 (4.5)	2 74. 7 (4.8)

as an iJJ ustration of why the SCMs simulated different clouds in the control climate.

5. Cloud Feedbacks

5.1. SCM Results at SU (Stratocumulus)

[21] We first use the cumulus under stratocumulus regime Sl 1 to esta blish a framework to interpret the cloud feed backs in the 15 SCMs. Figure 7 shows the change of net CRE from CTL to P2S at Sl l. Increase of CRE in the figure means positive cloud feed backs; decrease of CRE means negative feedbacks. For simplicity, the change of CRE is referred to as cloud feed back. The 15 SCMs simulated negative and positive cloud feedbacks that span a rather wide range of about 40 W/m^2. *Blossey et al.* [2013] showed this range as a bout 10 W/m^2 in LES models. Because of the simplified CGILS setup, we do not expect the feedbacks here to be the same as in the full GCMs, but they allow us to gain some insight into the physical processes that detemu ne them.

[2s] In Figure 7, the character "X" above a model's name indicates that shallow convection is not triggered in both the CTL and P2S sim ulations of t his model. The character "O" above a model's name indicates that shallow convection is active in at least one of the simulations of CTL and P2S. PBL schemes are always triggered in all mod els. Models without these characters about t hei r names used unified schemes of turbulence and shallow convection (such as CLUBB and RACMO) or did not subnu t informa tion for convection (such as ECMWF). One can see that models without active shallow convection tend to simulate negative cloud feed backs , while models with active convection tend to sim ula te positive cloud feed backs.

[29] Without convection, as discussed in the previous section for the JMA model, the water vapor balance is achieved by a competition between the moistening effect of the *"turb"* term in eq uation (7) and d rying effect of the net large-scale condensation *"c-e"* term and large-scale forcing; clouds are ca used by the moisteni ng term from the PBL scheme. Therefore, the response of the PBL scheme to SST largely determines the change of cloud water , hence, the cloud feed backs. Even tho ugh cloud microphysical and precipitation processes can also infl uence cloud feed backs, as mentioned before, since precipi tation is typically proportional to cloud wa ter, cloud wa ter controls the net change of condensates in the sim ulations.

[3o] The PBL moistening term at the alti tude of maxi-m um cloud liq uid water is larger in the warmer clima te in virt ually all models as shown in Figu re 8a. In the one exception of the CCC model, the sim ula ted alti tude of

Table 6. Same as Table 4 but for S6

M odel_ID	SH	LH	PREC	TG LWP	SWCR E	CRE
ACCESS	6.8 (2 0.4)	1 1 1.4 (10.9)	1.02 (0.1 6)	19.8 (0.9)	2 9.6 (2 0.4)	2 9.0 (2 0.4)
CA M4	8.5 (0.0)	I 05.3 (12.2)	0.00 (0.00)	247.9 (24.0)	2 177.4 (2 4.5)	2 160.1 (2 5.6)
CA MS	6.5 (2 0.2)	104.3 (13.4)	0.74 (0.1 6)	24.3 (2 3.4)	2 35.2 (8.2)	2 34.2 (8.1)
CCC	9.0 (0.5)	1 22.4 (7.3)	1.59 (0.60)	68.9 (2 34.2)	2 35.4 (24.9)	2 27.3 (18.7)
CLUBB	I 0.4 (2 0.1)	1 19.5 (10.2)	0.57 (2 0.10)	31.8 (2 0.6)	2 91.7 (1.4)	2 73.7 (2 0.1)
ECHAM6	2 5.6 (2 0. 7)	1 02.5 (9.2)	0.79 (0.00)	183.2 (8.2)	2 181.6 (2 0.1)	2 146.6 (2 4.1)
ECMWF	7.9 (0.6)	I 08.1 (8.5)	0.86 (0. 70)	25.5 (6.0)	2 12.6 (2 2.5)	2 7.1 (2 2.5)
EC_ETH	2.8 (2 1.2)	1 04.8 (7.6)	0.61 (0.1 0)	1 30.0 (5.0)	2 125.5 (2.8)	0.0 (0.0)
GFDL_A M3	8.8 (2 0.6)	1 10.0 (9.3)	0.84 (0.1 2)	5.9 (I. I)	2 12.7 (2 13.3)	2 1 1.7 (2 13.4)
GISS	1 1.4 (2 0.9)	125.6 (I 0.0)	1.41 (0.1 1)	18.8 (2 4.2)	2 41.9 (1 2.8)	2 39.4 (11.4)
GMAO	6.1 (2 1.9)	1 16.5 (6.1)	1.14 (0.1 1)	59.0 (1.3)	2 37.4 (1.0)	2 33.1 (0.8)
HadGEM2	6.0 (2 0.4)	1 09.9 (9.9)	0.98 (0.1 2)	3.7 (0.7)	2 22.0 (2 0.9)	2 20.1 (2 I. I)
IPSL	10.2 (2 0.5)	1 1 8.8 (10.7)	1.34 (0.1 7)	74.6 (2 1.6)	2 59.0 (4.7)	2 53.6 (4.0)
JMA	14.7 (2 0.1)	1 08.2 (7.8)	0.63 (0. 70)	179.8 (25.3)	2 107.0 (2 5.9)	2 101.2 (2 6.3)
RA CMO	12.0 (2 0.5)	I 08.2 (8.1)	0.66 (0.60)	63.2 (7.6)	2 28.4 (2 1.6)	2 25.8 (2 1.7)

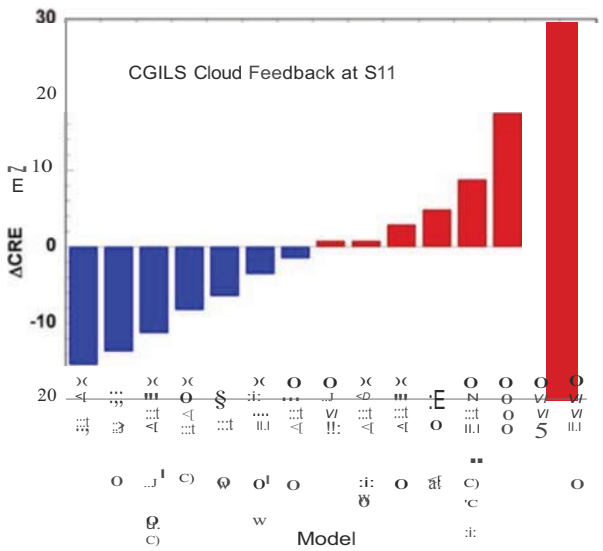

Figure 7. (a) Change of cloud-rad iative effect (CRE, W/m^2) in SCMs at location SI I corresponding to 2 K SST pert urbation. Character "X" above a model's name indicates that the shallow convection scheme is not active; "O" indicates that the shaJlow convection scheme is active. Models wi tho ut these characters ei ther do not separately parameterize shallow convection and PBL turbulence, or do not submi t results with convection informa tion.

maxim um cloud wa ter in P2S is m uch higher than in CTL, above the top of the boundary layer (not shown), where the turbulent term is small. The increased moistening by the PBL schemes is generall y consistent with the increase of surface latent heat flu x (LHF) in P2S, as shown in Figure 8b. The increase of latent heat fl ux wi th SST is consistent wi th CGILS LES sim ulations in *Blossey et al*. [20I3] (their Table 4) and in earlier LES studies under similar experimental setup [e.g., *Xu et al.,* 2010]. AJso, *Li ep ert and Pr evidi* [20I 2] showed that in virtually all 21 st century climate change simulations by CMIP3 models, surface latent heat fl uxes are larger i n a warmer clima te over the oceans (their Ta ble 2, column 3).

[3 1] Previous studies [e.g., *Caldwell and Bretherton*, 2009] have shown negati ve cloud feedbacks in mixed layer models (MLM) and have attribu ted the mechanism to la rger surface la tent heat fl ux and weaker large-scale subsidence i n a warmer climate. These two conditions are also shown in the CGILS SCM models that do not trigger convection. Table 5 shows that cloud wa ter path in the negative feed back models is increased in the warmer cljmate. The example in Figure 6a (dashed lines) for the TMA model also illustrates the larger moistening rate by turbulence and deeper cloud layer in the warmer clinrnte. The CGILS results are therefore consistent wi th the interpretation of the negative feed backs in MLMs. Exceptions are noted in wruch the convecti ve scheme is not acti ve in a model, but the model has small posi tive cloud feed backs, such as in CAMS and ECHAM6. These may be related with cloud-top entrainment, included explicitly and im plic-

Taking the ensem ble of models as a whole, we can use Figure 9a to schema tically summarize the negative cloud feed backs in the SCMs without convection. In these models, accompanied by the weaker large-scale subsidence, the warmer climate has greater surface latent heat flux, larger turbulence moisture convergence in the cloud layer, and consequently an inclination to give the negative cloud feedbacks. Tills mechanism is not new, but we see t hat it can explain the SCM resul ts in CGILS without activated convection.

[32] We now turn to models wi th active shallow convection. Figure 7 shows that these models tend to have positive cloud feed backs. As discussed in the previous section for CAM4 and GISS, shallow convection acts to dry t he cloud layer. It is a moist ure sink that has the same sign as the stratiform condensation sink in eq ua-

tion (7). The enhanced moisterung from the PBL scheme in the warmer climate is approximately balanced by enhanced drying from the sum of the stratiform condensation and shallow convection. If the rate of d rying from t he shalJ ow convection is greater than the rate of moistening from the PBL scheme as SST increases, the stra tiform condensation can decrease in a warmer clinrnte. This tends to reduce cloud water and clouds, thus causing positive cloud feedback. The enhanced rate of convective d rying in the warmer climate may be explained by the moisture flux in equation (4) immediately above the top of the boundary layer. The moist ure contrast is larger in the wam1er clima te, since the subsiding free tropospheric air remains dry but the total water in convective plumes increases with SST. An example is shown in Figure 6c for the GISS

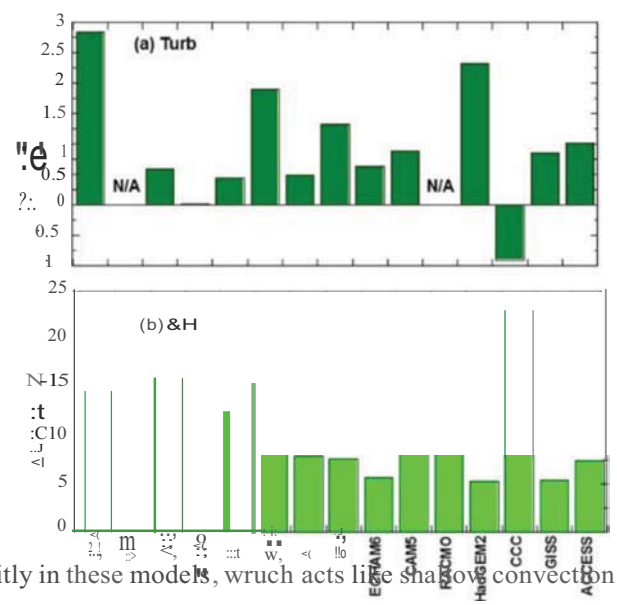

itly in these models, wruch acts lite shallow convection.

Model

Figure 8. (a) Change of moisture tendency in the layer of maximum cloud water {g/kg/day) by the "*Turb*" term from the control climate to the perturbed climate at SI 1. (b) Same as Figure 8a but for surface latent heat flux (W/m^2).

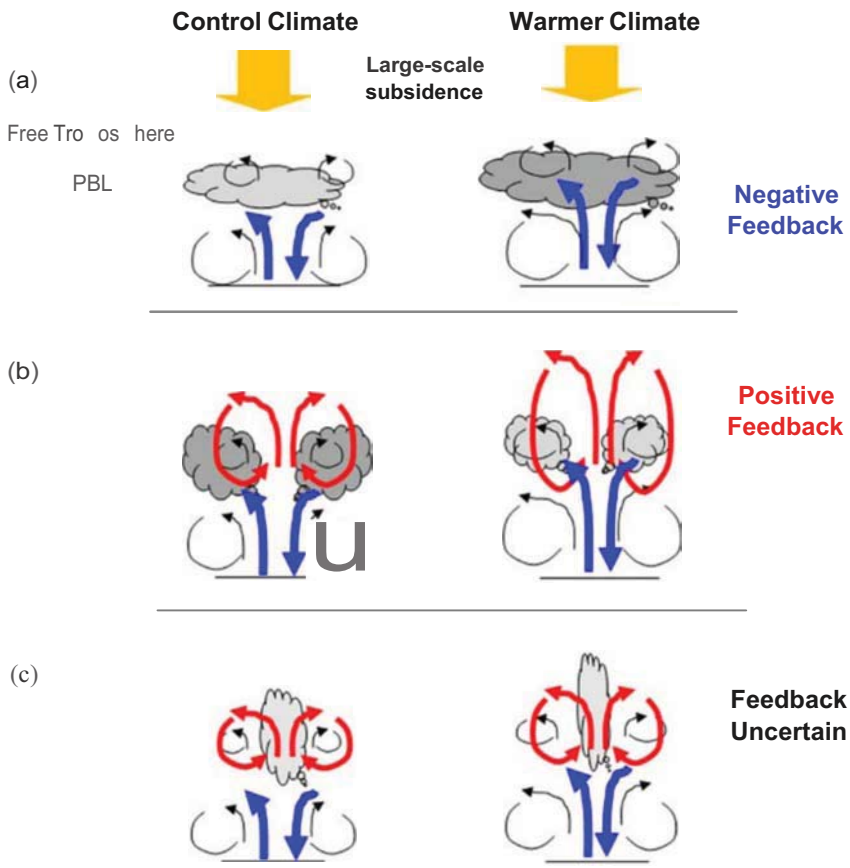

Figure 9. Schematics of cloud feed backs. Changes of clouds from the (left) control to (right) warmer clima tes. Blue arrows denote the term of turbulence parameterization in the moisture budget eq uation; red arrows denote shallow convection. The sizes of arrows schematically correspond to the magni tude of moisture tendency from the associated processes . (a) Negati ve cloud feed back, domina ted by the increase of surface turbulence, the "NESTS " negati ve cloud feed back mechanism (see text) . (b) Positive cloud feed back , domina ted by the increase of shallow convection or cloud-top entrainment, the "SCOPE " po si ti ve cloud feed back mechanism (see text). (c) Cloud feedback from shallow cumul us of sufficient depth, with sign depending on the cloud depth and lateral mixing.

model by using the dashed lines. In t he warmer climate, there is increase of t urbulence moistening, but larger increase of convective drying, and therefore red uced cloud water. Active convection therefore causes larger ventilation of the cloud layer in a warmer climate, which tends to decrease clouds and cause positive cloud feed backs. This increase of convecti ve mixi ng of boundary layer air together with the change of cloud -top entrainment ca uses more dil ution of the cloudy layer and therefore positive feedback. We can therefore use Figure 9b to schematically summarize the positive cloud feed backs in the models. The net cloud feed backs can be considered as due to two opposing roles of surface-based PBL t urbulence and shallow convection aided by cloud-top entrainment, wi th the latter dominating in most of the models in which convection is active. Figure 9b also applies to models wi th parameterizations of significant cloud-top entrainment. The PBL scheme can a lso be dominant over the shalJow convection scheme in some models, such as in CAM4. In this model, as discussed in the previou s section, the peak drying of shallow convection occurs below the cloud layer instead of within the cloud layer.

[33] *Brient and Bony* [2012] used t he larger moisture contrast between the free t roposphere and boundary layer in the warmer clima te to explain the positive cloud feedbacks in the IPSL SCM and GCM, while *Kawai* [2012] used the increased surface flux to explain the negative cloud feed back in the JMA SCM and GCM. These are consistent with the present interpretation. Figure 7 shows tha t in CGILS when con - vection is active, the positive feed back dominates the negative feedback. In GCMs or in the real atmospheres, any changes in the frequency of convection and convective mass fluxes would also matter. We call the a bove two competing mechan isms in Figure 9 as the "NESTS-SCOPE " (Nega tive feedback from Surface Tu rbulence under weaker Subsidence-Shallow Convection PositivE feedback) mechanisms . Obviously, given the wide range of physical parameterizations in models, this in terpretation may not fit all mod els. For exam ple, *Zhang and Br etherton* [2008] showed that in CAM3 the interaction of an unintended deep convection with the cloud microphysical scheme caused a negative cloud feedback in tha t mod el. Nevertheless , the delineation of the two

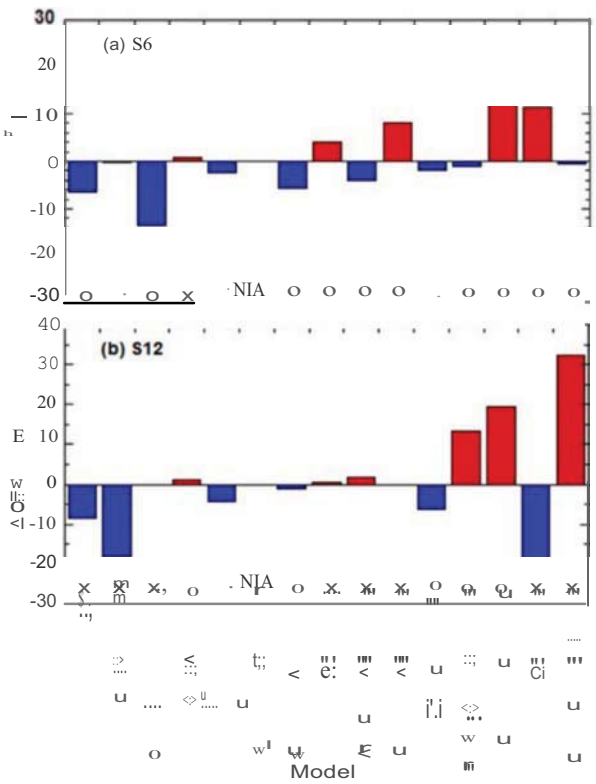

Figure 10. Same as Figure 7, but for (a) S6, (b) Sl 2. The models are ordered in the same sequence as in Figure 7. One model (EC_ECH) did not reach quasi-equilibrium state and it is ind icated by *"NIA"*.

competing mechanisms is a useful framework to interpret the majori ty of models.

5.2. SCM Results at S6 (Shallow Cumulus) and at S12 (Coastal Stratus)

[34] We now use the same framework as we used for Sl 1 to interpret SCMs results at the other two locations. Before proceeding, we need to supplement our schematics with another scenario in which the depth of convection is large and mixing of cloud y ai r with dry air can occur la terally . If the cloud-scale dynamical fields and the environmental relative humidity are the same, larger d rying from convection is expected in P2S than CTL because of the larger difference of the absolu te h umidity of moist ure across cloud lateral bounda ries just like across cloud tops. This is schematically shown in Figure 9c. Other factors such as cloud -scale dynamics, cloud depth , and cloud microphysics can also change in a warmer climate, leading to more complicated behavior of clo ud feed backs for t hicker clouds. This scena rio also incl udes regime change of clouds from stratocumul us to shallow cum ul us as exhibited by some models (e.g., CCC at Sl 1, not shown).

[3s] Figure lOa shows the SCM cloud feedbacks at the shallow convection location S6, wi th a range of a bout 30 W/m^2 (in LES, models , the range is less t han 3 W/m^2). The models a re ordered in the same seq uence as in Figure 7. Almost all model s sim ulated convection at due to the com plications described above, convection at S6 does not necessarily correspond to posi tive cloud feed backs. In au sim ulations, surface la tent hea t flux is greater in the warmer climate (Table 6). We may therefore use the same framework as for Sl 1 to think tha t the larger surface latent heat flux alone is a factor for more clouds in a warmer climate, but the other factors from shallow convection such as la teral mixing favor more dil ution of clouds and a positive cloud feed back . The two effects compensa te each other d ifferently in the mod els beca use of the different assumptions in the specific parameterizations.

[36] Figure l Ob shows SCM results at S12, where SST is colder and subsidence is stronger than at Sl 1. The corresponding changes of surface turbulent fluxes and cloud water path are given in Ta ble 5. Clouds a re restricted to wi thin the boundary layer. The sim ulated cloud feedbacks also span a wide range. Three models simulated no clouds at this location (GFDL AM3, EC-ETH, and CAMS) (due to the constancy of forcing). Most models simulated the same cloud feed back signs as at Sl 1. Some sim ulated opposite signs, one of which S6. Cloud feed backs are generally consistent with the change of cloud liquid water path (Table 6). Partially

is the GISS model. As indicated by the "X" character above the GISS model in Figure lOb, for this model, shallow convection is not active at Sl 2, in contrast to be active a t S l 1. Consistent wi th our hypothesis, the cloud feed back changed from positive to nega tive. The concept ual framework i n Figures 9a and 9b can be gen - erally applied to describe the behavior of cloud feed- backs in the SCMs at Sl2.

5.3. LES Results

[37] The CGILS LES result s have been sum marized in *Blossey et al.* [2013]. To compare wi th SCM results, in Figu res l l a-1lc, we show the LES cloud feedbacks at the three locations of S6, S ll , and Sl 2, respectively . The LES results are more consistent with each other than SCMs. A t the shallow cumulus location S6 (Figure l l a), LES model s simulated a smalJ po sitive cloud feed- back except for DA LES and WRF that had negligi ble feedbacks. A t the stratocum ulus location Sl 1 (Figure 11b), all models except for SAM simulated positive cloud feedbacks. At the coastal stratus loca tion S12 (Figure 1l c), all except for DALES simulated negative cloud feed back. There is therefore consensus, but not uniform agreement, among the LES models wi th regard to simulated cloud feedbacks.

[3s] *Blossey et al.* [2013] a ttributed the negative feed- back at S12 to the deepening of the cloud layer in a rela- tively well-mixed boundary layer that is related to weaker large-scale subsidence in the wam1er climate. As mentioned before , this is also the interpreta tion of MLM negative cloud feedback and in the SCMs of CGILS as shown in Figure 6a. In some SCMs, vertical resolutions are not sufficient, so the d eepening of clouds cannot be simula ted. In these models, the weaker subsi- dence leads to less su bsidence d rying in the warmer cli- ma te. This i s accom panied by larger turbulent convergence of moistu re into the cloud layer from enhanced surface flux and more liquid water. Therefore , the SCM interpretations are still consistent with the

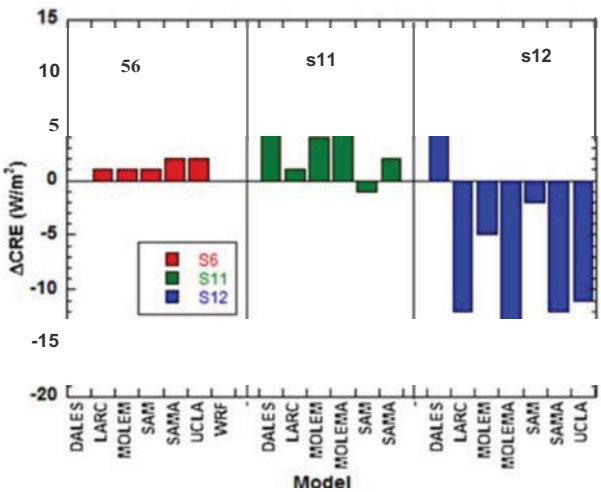

Figure 11. Same as Figure 7 but in LES models. (a) S6, (b) SI I, and (c) S12.

LES results of deepening boundary layer. At Sl **1,** *Blossey et al.* [20 13] attributed the positive feed back in the LES models to cloud thinning in a warmer climate ca used by decoupling of the boundary layer with the stratocumulus layer. In SCMs, the decoupled mixing is calc ulated by ei ther shallow convection or cloud-top entrainment or both, which has been shown to ca use positive cloud feed backs as in Figure 6c. At S6, *Blossey et al.* [2013] attrib uted the posi ti ve feedback to more preci pitation.

[39] A companion paper by *Br etherton et al.* [2013] investigated the sensi tivity of LES res ults to large-scale conditions, incl uding separate changes in su rface forcing, large-scale subsidence, environmental rela tive h umidity , and $C0_2$ concentration. These are not studied here since in CGILS we onl y aim at the total derivate of cloud feedback to imposed SST forcing with implied change in large-scale subsidence. The potential im pact of the chan ge of $C0_2$ forci ng is left for future stud y. We point out that the consensus among the LES models in Figure **11** does not necessarily mean they simulated the correct cloud feed backs. Nevertheless , they give pla usible answers for SCMs to target for. Event ually, they need to be validated by observations under more realistic experimental set ups.

6. Summary and Discussion

[4o] The experimental setup of CGILS was used to simulate shallow cumul us, stratocumulus, and coastal strat us and to investigate the physical mechanisms of cloud feedbacks under idealized climate change i n single column models. In models where shallow convection is not activated or plays minor role in drying the cloud layer, cloud feed backs tend to be negative . In models when convection is active, cloud feed backs tend to be posi tive in the stratocumu l us and coastal stratus regime , but uncertain in the shallow cum ulus regime. A framework is described to interpret the SCM cloud feedbacks by using the two opposing effects of increased moistening from **PBL** scheme under weaker large-scale subsidence and enhanced drying from shallow convection in a warmer climate, with the former ca using negative cloud feed backs and the convective scheme ca using positive cloud feedbacks. The convective scheme plays a more dominant role at times when it is active. These mechanisms are sunlJDarized as the NESTS nega tive feed back and SCOPE positive feed back mechanisms. LES models simulated overall consistent positive cloud feed backs in the shallow cum ul us and stratocum ulus regimes, but negative feed backs in the coastal stratus regime. The LES results tend to support the NESTS-SCOPE mechanisms.

[41] The relevance of CGILS results to cloud feedbacks in GCM s and in real-world climate changes is not clear yet. In a preliminary comparison to cloud feedbacks in four GCMs a t the three loca tions, SCMs results were uncorrelated to those simulated by the parent GCM, suggesting the complexity of translating the results from SCMs to the feedbacks sim ulated by GCMs. While CGILS is motivated by understanding the physical mechanisms of cloud feedback s in GCMs, there are several issues that limit the applicability of the SCM results . First, the idealized forcing is steady state. Diurnal and synoptic variabilities are not considered. Second, the large-scale fields are not interactive wi th clouds. Third, the spatial variability of GCM cloud feed back may be la rge and so direct comparison a t the selected locations may be inappropriate. Furthermore, the pattern of atmospheric large-scale condition in the GCMs may shift locations in a warmer climate *[Webb and Lock,* 2012]. Future phases of CGILS will investigate how results from the sin1plified case stud y should be used or how the case study should be modified to better understand cloud feedbacks in more complex model s and in observations. The CGILS results highlight the desira bility to treat physical parameteriza tions in General Circulation Models (GCMs) as an integrated system rather than individual components in order to red uce cloud feed back uncertainties.

[42] Acknowledgments. We thank two anonymous reviewers whose comments have led to a significant improvement of this paper. Sung-bi n Park of the Seoul National University (SNU) participated in the initial phase of the CGILS project. His tragic death disrupted the submission of results from the SNU model. This paper serves as an appreciation and memory of him. Zhang's CG I LS resea ·ch is supported by the Biologica l and Environmental R esearch Dl v1s1on m the Office of Sciences of the US Department of Energy (DOE) through 1ts FASTER project , by the NASA Modeling and Analysis Program (MAP) and the US National Science Fotmdation to the Stony Brook University. Bretherton and Bl ossey acknowledge support from the NSF Center for M ultiscale M odeling and Predictio n , A ustin is supported by Canada 's NSERC. Del Genio is support ed by the NASA MAP program. V. Larson gratefully acknowledges support from the National Science Foundation (grant AGS-0968640) and the US Department of Energy (grant DE-SC0006927). Wolf was supported by the DOE ASR program. Webb was supported by the Joint DE CC/ Defra Met Office Hadl ey Centre Clima te Program (GAOi 101) and funding from the European Union , Seventh Framework Program (FP7/2007-201 3) under grant agreement number 244067 via the EU Cloud Intercomparison and Process Smdy Evaluation Project (EUCL IPSE). Franklin was suppor ted by the Australian Ch mate Change Science Program, funded jointly by the Department of Chmate Change and Energy Efficiency , the Bureau of Meteorology and CSIRO. Hens was funded by the Deutscher Wetter Dienst (DWD)

through the Han s-Ertel Centre for Weather Resea rch, as part of the EUCLIPSE project under Framework Program 7 of the European Union. The simulations with the Dutch LES model were sponsored by the National Computing Facilities Foundation (NCF). The National Center for Atmospheric R esearch is sponsored by the National Science Foundation.

References

And rews , T., *1.* M. Gregory , M . J. Webb, and K. E . Taylor (2012), Forcing , feedbacks and climate sensi tivity in CM CP5 coupled atmosphere-ocean climate models, *Geophys. Res. Lett ., 39,* L097 l 2, doi:I0.1029/2012GL051607.

Blossey, P. N ., C. S. Bretherton, M. Zhang, A. Cheng, S. Endo , T. Heu s, Y. Li u, A. L ock, S. R . de Rood e, and K.-M. Xu (2013), Marine low cloud sensitivity to an idealized climate change: The CGI LS L ES lntercomparison, *./. Adi •. Model. Earth Sys t., 5,* 234-258, doi :I 0.1002/jame.20025.

Blossey, P. N. , C. S. Bretherton , and M. C. Wyant (2009), Understanding subtropical low clo ud response to a warmer clima t e in a superparameteri zed clima te model. Part II : Column modeling with a cloud-resolving model , *./. At!i>. Mod el. &,,.th Sys t., I ,* 8, 14 pp., doi : 10.3894/JAMES.2009.1.8.

Bretherton, C. S., and S. Park (2009) , A new moist t tu-bulence parameterization in the community atmosphere model , *./. Clim., 22,* 3422-3448, doi:IO.l 175/2008JCLI2556.I.

Bretherton, C. S., P. N . Blo ssey, and C. R . Jones (201 3), A large-eddy sim ul ation of mechanisms of botmdary layer cloud response to climate change in CGILS, *.!. Adi •. Model. &1rth Syst .,* doi: I 0.1002/ jame .20019, in press.

Brink op, S., and E . Roeckner (1 995), Sensitivity of a general ci rculation model to parameteri za ti ons of cloud -mrbulence interactions in the atmospheric boundary layer, *Tellus, Ser. A , 47,* 197-220.

Bon y, S., and J .-L. Dufresne (2005), Marine boundar y layer cl ouds at the heart of cloud feedback uncertainties in climate models, *Geoph ys. Res. Lett., 32,* L20806, doi:10. 1029/2005GL02385 l .

Bon y, S., and K. A. Emanuel (2005), On the role of moist processes in tropical intraseasonaJ variabili ty: Cloud-radiation and moistll reconvection feedbacks, .!. *Atmos.* Sci. , *62,* 2770-2789 , doi:I 0.1 175/ JAS3506. I.

Bon y, S., et al. (2006) , H ow well do we understand climate change feedback processes? *./. Clim., 19,* 3445-3482.

Brient, F., and S. Bony (201 2), Interpretation of the positive low cl oud feedback predicted by a climate model und er global warming , *Clim. Dy11., 6,* 1-17, doi:I0.1007/s00382-01l-1279-7.

Caldwell , P., and C. S. Bretherton (2009), Response of a subtropical stratocumulus-capped mixed layer to climate and aerosol changes, .!. *Clim.,22,* 20-38.

Cess, R . D., et al. (1990) , Intercomparison and interpretation of cloud-climate feedback processes i n nineteen atmospheric general circulation models,.!. *GeophJl. . Res., 95,* 16,601-16,615.

Dee, D. P., et a l. (201 1), The ER A-Interim reanalysis: Configuration and performance of the data assimilation system, *Q. J. R. M eteorol. Soc., 137,* 553-597, doi:I 0.1002/qj.828.

Del Genia , A. D., and M. Yao (1993), Efficient cum ul us parameterization for long-term climate smdies: The GISS scheme, i n *The R epresentation of Cumulus Convection in Numerica l Models,* vol. *46,* Meteorological Monographs, edited by K . A. Eman uel and D. A. Raymond, pp. 181-184, Am. Meteorol. Soc., Orlando , Fla.

Del Genia , A. D., M.-S. Yao, and J . Jonas (2007), Will moist convection be stronger in a warmer climate? *Geophys. Res. Lett., 34,* L 16703, doi:IO. I029/2007GL030525 .

Del Genia , A . D., M.-S. Yao , W. Kovari , and K . K .-W. Lo (1996), A prognostic cloud water parameterization for globa l climate models. *.!. Clim, 9,* 270-304, doi:IO. I 175/1520-0442(1996)009<0270:APCWPF> 2.0.C0;2.

Donner , L. J ., et al. (201 1), The dynamica l core, ph ysical parameteri zations, and basic simulation characteristics of the atmospheric component A M3 of the G FDL global coupl ed model CM3, *.!. Clin1., 24,* 3484-3519, doi:I0.1 175/201 IJCLI3955. I.

Emanuel , A. K . (1991), A scheme for representing ctmrnl us convection in l arge-sca le models, *./. Atmos. Sci., 48,* 2313-2329, doi:I 0.1175/ 1520-0469(1991)048<23 I 3:ASFRCC>2 .0.C0;2.

Emanuel , A. K . (1993), A cumulus representation based on the episodic mixing model: the importance of mixi ng and microphysics in predicti ng h1m1idity. *AM S M eteorol Monogr 24(46),* 185-192.

Endo, S., Y. Liu , W. Lin , and G. Liu (201 1), Extension of WRF to cloud-resol ving simulations driven by large-scale and surface forcings. Part I: Model configuration and validation , *Tech Note BNL-96480-2011-.IA,* Brookha ven Natl. Lab., New York. [Avai lable at http:// www .bnJ .gov/envsci/pubs/pdf/201 3/BNL-96480-201 1-JA.pdf.].

Galaz, J.-C ., V. E . Larson, and W. R . Cotton (2002a), A PDF-ba sed model for boundary layer cl ouds. Part I: Method and model description, *J. Atmos. Sci , 59,* 3540-3551 , doi: 10.1 175/1520-0469 (2002)059 <3540:A PBM FB>2.0.CO;2.

Galaz, J.-C. , V.E. Larson , W.R. Cotton (2002) , A PDF-Ba sed Mod el for Bound ary Layer Cloud s. Part II : Model Results. *./. Atmos . S ci., 59,* 3552-3571. doi: http://dx.doi.org/ I0.1 175/ 1520-0469(2002)059 <3552:A PBM FB >2.0.C0;2.

Galaz, J.-C., V . E. Larson, J . A . Han sen, D. P. Schanen , and B. M . Griffin (2007), Elucidating model i nadeq uacies in a cloud parameterization by u se of an ensemble-based calibration framework , *Mon. Weather R ei•., 135,* 4077-4096 , doi: I O. l l 75/2007MWR2008. I .

Grant, A. L. M. (2001), Cloud-base !luxes in the ctmrnlus-capped botmdary layer, *Q. .!. R. Meteorul. Soc., 127,*407-421.

Gregory , D., and P. R . R . R own tree (1990), A mass llux convection scheme with representation of cloud ensemble characteristics and stability dependent closure, *Mon. Weather Rei•., 118,* 1483-1 506.

Hack , J. *1.* (1994), Parameterization of moist convection in the Nati onal Center for Atmospheric Research comm unity climate model (CCM2), *./. Geophys. Res., 99,* 5551-5568.

Heu s, T., et al. (2010), Formulation of the Dutcll atmospheric l arge-edd y simulation (DA LES) and overview of its applications, *Geosci. Model D ev., 3,* 41 5-444, doi: I 0.5194/gmd-3-415-2010.

Hewitt, H . T., D. Copsey, I. D. Cul verwe ll, C. M. Harris, R . S. R . Hill, A. B. Keen , A. J. McLaren , and E. C. Hunk e (201 1), Design and implementation of the infrastructme of HadGEM3: The next generation Met O!Tice climate modelling system, *Geosci. Model De1•., 4,* 223-253.

Holtslag, A. A . M., and B. A. Bovil le (1993), Local versus nonlocal boundary-layer diffusion in a global climate model , *J. Clim., 6,* 1825-1 842, doi:I 0. 1 175/ 1520-0442(1 993)006< 1825:L VNBLD> 2.0.C0;2.

Holtslag, A. A. M., and C.-H. Moeng (1991), Eddy diffusivity and coun - tergradient transport in the convective atmospheric boundary layer, *./. Atmos. Sci , 48,* 1690-1 698, doi:I 0.1 175/1520 -0469(1991)048 <1690: EDACTI>2 .0.C0;2.

Hourdin , F., et al. (2006), The LM DZ4 genera l circulati on model: Climate performance and sensitivit y to parametrized physics with emphasis on tropical convecti on, *Clim. Dyn. ,* 27(7), 787-813.

Isotta, F. A., P. Spichtinger, U. Lohm ann, and K . van Salzen (201 1), Improvement and implementation of a parameteri zation for shallow cumu lus in the global climate model ECHAM5-HA M, *.!. Atmos. S ci., 68,* 515-532.

JMA (201 3), Outli ne of the opera tiona l numerical weather prediction at the Japan Meteorological Agency , Appendix to WMO *Tech Prog. Rep. on the Globol Data-Pro cessing and Forecosting Sys tem and Numerical Weather Pr ediction Resear ch,* Jpn. Meteorol. Agen cy, Tok y o. [Available at http://www.jma.go.jp/jma/jma-eng/jma-center/ nwp/outline2013-n wp/i ndex .htm.].

Kato , S., et al. (201 1), Impro vements of top-ol atmosphere and surface irradiance com putations with CA LI PSO, CloudSat , and MODIS-derived cloud and aerosol properties, *./. Geophys . Res., 116,* D 19209, doi:I 0.1029/2011 JDO1 6050.

Ka wai , H . (201 2), Examples of mechanisms for negative cloud feedback of stratocumu lus and stratus in cloud parameteri zations, *SOLA ,8,* 1502 154, doi:I 0.2151/sola .2012-037.

Khairoutdino v, M. F., and D. A . Randall (2003), Cloud-resolving modeling of the A RM summer 1997 IOP: Model form ulation , result s, uncertainties and sensiti vities , *./. Atmos. Sci., 60,* 607-625.

Larson, V. E., and J.-C . Galaz (2005), Using probabili ty density function s to derive consistent closure relationshi ps among higher-ord er moments , *Mon. Weather Rei•., 133,* 1023-1042.

Liepert, B. G., and M . Previdi (201 2), Inter-model variability and biases of the global water cycle in CM IP3 coupled climate models, *E111iron. Res. Lett.,* 7, 014006, doi:I0.1088/1748-932617/ I/014006.

Lock , A. P. (2009), Factors infl uenci ng cloud area at the capping inversion for shallow cumulus clouds, *Q. J. R Meteorol. Soc., 135,* 941-952, doi:10.1002/qj.424.

Lock , A. P., A. R. Brown , M. R. Bush , G. M. Martin , and R. N. B. Smith (2000), A new boundary layer mixing scheme. Part **I:** Scheme description and single-<:olumn model tests, *Mon. Weather Rev., 128,* 3187-3199, doi: 10.1 175/15200493(2000) 128<3187:ANBLMS>2.0.C0;2.

Louis, J., and J. Geleyn (1982). A short history of the PBL parameterization at ECMWF. Proc. ECMWF Workshop on Planetary Boundary Layer Parameterization , *Reading, United Kingdom, ECMWF,* 59-80.

Ma , X. , K. von Salzen, and J. Cole (201 0), Constraints on first aerosol indirect effect from a combination of MOD!S-CER ES satellite data and global climate simulations, *Atmos. Chem. Phys., JO,* 9851-9861. [Available at http://www .doaj.org/doaj?funcS openurl&genreS article&issnS l 6807367&date5 201O&volumeS 1O&issueS 6&spage5 13945.J.

Marti n, G. M., N. Bellouin , W. **J.** Collins, l. D. Culvenvell, P. R. Halloran , S. C. Hardiman , T. J. Hinton , and C. D. Jones (20 l 1), The HadGEM2 family of Met Office Unified Model climate configurations, *Geosci. Model De 11., 4,* 723-757, doi: 10.5194/gmd-4-723-201 1 .

Mellor , G. L., and T. Yamada (1974) , A hierarchy of turbulence closure models for planetary boundary layers, .! *Atmos. Sci., 31,* 1791-1806, doi: 10.1 175/1520-0469(1974)031 <1791 :AHOTCM>2.0.C0;2.

Mlawer , E. J. , S. J . Taubman , P. D. Brown, M. J . Iacono , and S. A. Clough (1997), RRTM: A validated correlated-k model for the long-wave, *.l. Geophys. Res., 102,* 16,663-16,682.

Molod , A., L. Takacs, M. Suarez, J. Bacmeister , I-S. Song, A. Eichmann, Y. Chang (2012), The GEOS-5 Atmospheric General Circulation Model: Mean Climate and Development from M ER RA to Fortuna . NASA Technical R eport Series on Global Modeling and Data Assimilation , *NASAITM-2008-104606 , 28,* 1 15.

Moorthi , S., and M. J. Suarez (1992), Relaxed Arakawa-Schubert: A parameterization of moist convection for general circulation models, *Mon. Weather Rev., 120,* 978-1002, doi:l0.1 17511520-0493(1992) 120 <0978:R ASAP0>2.0.C0 ;2.

Neale, R. B., et al. (2010), Description of the NCA R Community Atmospheric Model (CAM5.0), NCAR/TN 486 1STR. [Available at http://www .cesm.ucar.edu/models/ccsm4 .O/cam/docs/descri pt ion/ cam4_desc.pdf .].

Neale, R. B., et al. (2012), Description of the NCA R Community Atmospheric Model (CAM5.0), NCAR/TN 486 1STR. [Available at http://www .cesm.ucar.ed u/models/cesm 1.0/cam/docs/descri pt ion/ cam5_desc.pdf.].

Neggers, R. A. J ., M. Koehler, and A. A. M. Beljaars (2009a) , A dual mass n ux framework for boundary-layer convection. Part I: Transport , .! *Atmos. Sci. , 66,* 1465-1487 , doi: 10.1 1 75/2008JAS2635 .l.

Neggers, R. A. J. (2009b), A dual mass nux framework for boundary-layer convection , Part fl: Clouds, .! *Atmos. Sci., 66,* 1489-1506, doi: **10.1** 1 75/2008JAS2636. l.

Pan, D.-M ., and D . Randall (1998), A cumulus parameterization with a prognostic closure , *Q. .!. R. Meteorol. Soc. , 124,* 949-981.

Park , S., and C. S. Bretherton (2009), The Universi ty of Washington shallow convection and moist tl1rbulence schemes and their impact on climate simulations with the community atmosphere model , *.!. Clim., 22,* 3449-3469, doi: lO. l 1 75/2008JCLI2557. l.

Ramanathan , V., R . D. Cess, E. F. Harrison, P. Minnis, B. R . Barkstrom , and D. L. Hartmann (1989), Cloud-radiative forcing and climate: Results from the Earth Radiation Budget experiment, *Science, 243,* 57-63.

Randall , D. A., and D. G. Cripe (1999), Al ternative methods for specification of observed forcing in single-column models and cloud system models , .! *Geophys. R es., 104(020) ,* 24,527-24 , 545, doi: 1 0.1 029/ 199910900765.

Randall , D. A., et al. (2007), Climate models and their evaluation , in *Climate Change 2007: The Scient[/ic Basis ,* edited by S. Solomon et al., pp. 589-662, Cambridge Univ. Press, Cambridge, U. K .

Rienecker, M .M ., et al. (2008), The GEOS-5 Data Assimilation System Documentation of Versions 5.0.l and 5.1.0, and 5.2.0. NASA Technical Report Series on Global Modeling and Data Assimilation , *NASAITM-2008-104606 , 27,* 92.

Schmidt, G. A., et al. (2006) , Present day atmospheric simulations using GISS Mode!E: Comparison to in-situ, satell ite and reanal ysis data , *J. Clim., 19,* 153-192.

Siebesma , A. P., et al. (2004), Cloud representation in general circulation models over the north ern Pacific Ocean: A EUROCS i ntercomparison stt1dy, *Q. .!. R Meteorol. Soc., 130,* 3245-3267.

Sobel , A ., J . Nilsson, and L. Polvani (2001), The weak temperatt1re gradient approximation and balanced tropical moim1re waves, *.!. Atmos. Sci., 58,* 3650-3665.

Soden , B. J., A. J. Broccoli , and R . S. Hemler (2004), On the use of cloud forcing to estimate cloud feedback, *J. Clim., 17,* 3661-3665.

Stevens, B., et al. (2005), Eval uation of large-edd y simulations via observations of nocturnal marine stratocumulus, *Mon. Weather Rev., 133,* 1443-1462.

Stevens, B., et al. (201 3), The atmospheric component of the MPI-M earth system model: ECHAM6 , *J. Adv. Model. Earth Syst ., 5,* 146-172, doi:10.1002/jame.2001 5.

Stevens, B., and A. Seifert (2008), Understandi ng macrophysical outcomes of microphysical choices in simulations of shallow cumulus convection,]. *M eteorol. Soc.Jpn. A, 86,* 143-162.

Teixeira , J., et al. (201 1), Tropical and subtropical cloud transitions in weather and cl imate prediction models: The GCSS/WGNE Pacific cross-section intercomparison (GPCI) , *J Clim., 24,* 5223-5256, doi : 10.1 175/201 IJCLI3672. l.

Tiedtke, M. (1989), A comprehensive mass nux scheme for cumulus parameterization in large-scale models, *Mo11. Weather Rev., 117,* 1779-1800, doi: 10. **l**1 75/1520-0493(1989)1 17<1779:ACMFSF>2.0. C0;2.

von Salzen , K., and N. A. McFarlane (2002), Parameterization of the bulk effects of lateral and cloud-top entrainment in transient shallow cumulus clouds, *.!. Atmos. Sci., 59,* 1405-1430, doi: 10.**l** 1 75/1520-0469(2002)059<1405:POTBE0>2.0.C0;2.

von Salzen , K., et al. (20 13), The Canadian Fourth Generation Atmospheric Global Climate Model (CanAM4). Part I: Representation of physical processes, *Atmosphere, 51,* 104-125, doi:10.1080/ 07055900.2012. 755610.

Webb, M . J. , and A. Lock (2012), Coupling between subtropical cloud feedback and the local hydrological cycle i n a cl imate model, *Clim. Dy11. , 27,* 17-38, doi: 10.1007/s00382-01 2-1 608-5.

Xu , K .-M., and A. Cheng (201 3), Evaluating low cloud simulation from an upgraded multi scale modeling framework . Part II: Seasonal variations over the Eastern Pacific, *.!. Clim., 26 ,* 5741-5760, doi: 1 0.1 175/JCLI-D-1 2-00276.1.

Xu , K.-M., A. Cheng, and M. Zhang (2010), Cloud-resolvi ng simulation of low-cloud feedback to an increase in sea surface temperattll"e, *.!. Atmos. Sci., 67,* 730-748.

Zelinka , M. D., S. A. Klein , and D. L. Hartmann (201 2), Computing and partitioning cloud feedbacks usi ng cloud property histograms. Part I: Cloud radiative kernels , *J. Clim., 25,* 3715-3735, doi: 1 0.1 175/ JCLI-D-1 1-00248.1.

Zhang, M ., and C. S. Bretherton (2008), Mechanisms of low cloud climate feedback in idea lized single-column simulations with the Community Atmospheric Model (CA M3), *J. Clim., 21,* 4859-4878.

Zhang, M. , et al. (2012), CGILS: An experimental design to study low cloud feedbacks in general circulation models by using si ngle-column and large eddy simulation models, *.!. Ad v. Model. Earth Syst., 4,* M 12001, doi:l0. 1029/201 2MS000182.

Zhao, M., l. M. Held , S.-J. Lin , and G. A. Vecchi (2009) , Simulations of global hurrican e climatology , interannual variability , and response to global warming using a 50-km resolution GCM, *.!. Clim., 22,* 6653-6678, doi: 10.1175/2009JCLI3049.l.